



저작자표시-비영리-변경금지 2.0 대한민국

이용자는 아래의 조건을 따르는 경우에 한하여 자유롭게

- 이 저작물을 복제, 배포, 전송, 전시, 공연 및 방송할 수 있습니다.

다음과 같은 조건을 따라야 합니다:



저작자표시. 귀하는 원저작자를 표시하여야 합니다.



비영리. 귀하는 이 저작물을 영리 목적으로 이용할 수 없습니다.



변경금지. 귀하는 이 저작물을 개작, 변형 또는 가공할 수 없습니다.

- 귀하는, 이 저작물의 재이용이나 배포의 경우, 이 저작물에 적용된 이용허락조건을 명확하게 나타내어야 합니다.
- 저작권자로부터 별도의 허가를 받으면 이러한 조건들은 적용되지 않습니다.

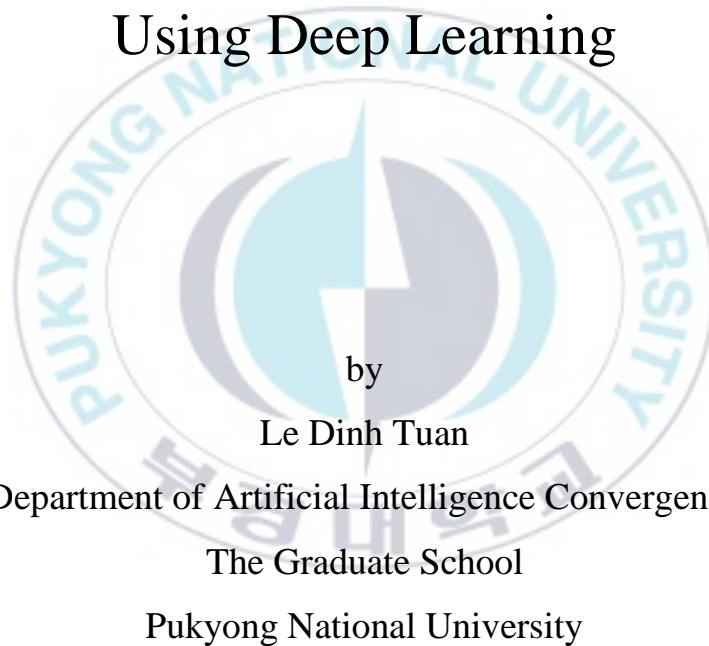
저작권법에 따른 이용자의 권리는 위의 내용에 의하여 영향을 받지 않습니다.

이것은 [이용허락규약\(Legal Code\)](#)을 이해하기 쉽게 요약한 것입니다.

[Disclaimer](#)

Thesis for the Degree of Master of Engineering

COVID-19 Detection and Severity
Grading with Chest-Xray and CT-Scan
Using Deep Learning



by

Le Dinh Tuan

Department of Artificial Intelligence Convergence

The Graduate School

Pukyong National University

February 2023

COVID-19 Detection and Severity Grading with
Chest-Xray and CT-Scan Using Deep Learning
딥러닝 방법을 사용한 흉부 X-선 및 CT 스캔을
통한 COVID-19 검출 및 심각도 등급 판별

Advisor: Prof. Ki-Ryong Kwon

by

Le Dinh Tuan

A thesis submitted in partial fulfillment of requirements for
the degree of

Master of Engineering

in Department of Artificial Intelligence
The Graduate School, Pukyong National University

February 2023

COVID-19 Detection and Severity Grading with Chest-Xray and
CT-Scan Using Deep Learning

A thesis

by

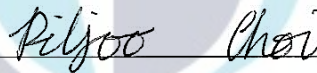
Le Dinh Tuan

Approved by:



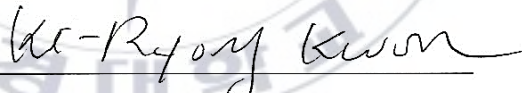
(Chairman)

Prof. Suk-Hwan Lee



(Member)

Prof. Piljoo Choi



(Member)

Prof. Ki-Ryong Kwon

February 17, 2023

Contents

요 약	vi
Abstract.....	vii
I. Introduction	1
1.1 Coronavirus pandemic (COVID-19).....	1
1.2 Deep Learning for Medical Images Analysis.....	2
1.3 Outline of Thesis	4
II. Related Works	5
2.1 COVID-19 Detection Using Chest X-Ray	5
2.2 COVID-19 Detection Using CT-Scan.....	6
2.3 COVID-19 Severity Grading Using Chest X-Ray	7
III. The Proposed Methods and Results	10
3.1 Dataset	10
3.1.1 COVID-19 Detection Chest X-Ray Dataset	10
3.1.2 COVID-19 Detection CT Scan Dataset	11
3.1.3 COVID-19 Severity Grading Dataset	14
3.2 Deep Learning Architectures.....	15
3.2.1 DenseNet121	16
3.2.2 ResNet50	17
3.2.3 InceptionNet.....	18
3.2.4 Swin Transformer.....	19
3.2.5 EfficientNet	20
3.2.6 Hybrid EfficientNet and DOLG.....	22

3.3 Preprocessing and Training Setting.....	23
3.3.1 Data Augmentation	23
3.3.2 Hardware and Hyperparameter Setting.....	24
3.4 Evaluation Metrics	25
3.4.1 Precision Metric	26
3.4.2 Recall Metric	26
3.4.3 F1-score Metric	26
3.4.4 Macro-Average Metric.....	27
3.4.5 Macro-Average Metric.....	27
3.5 Results and Discussion.....	28
3.5.1 COVID-19 Chest X-Ray Classification Results	28
3.5.2 COVID-19 CT Scan Classification Results	34
3.5.3 COVID-19 Chest X-Ray Severity Grading Results.....	37
3.5.4 Limitations of this study.....	42
IV. Conclusion.....	45
References	46
Acknowledgement	52

Figures

Fig. 1. Coronavirus PCR-RT Testing.....	1
Fig. 2. Apply Deep Learning for Medical Image Classification.	3
Fig. 3. Chest X-Ray for COVID-19 Detection.....	5
Fig. 4. CT Scan Images apply for COVID-19 Detection.	7
Fig. 5. COVID-19 Severity Assessment Using Chest X-Ray Images.....	8
Fig. 6. DenseNet121 overall architecture.....	16
Fig. 7. ResNet50 Model Architecture	17
Fig. 8. InceptionNet module with dimensionality reduction.....	19
Fig. 9. Swin Transformer with Shifted Window Architecture.....	20
Fig. 10. EfficientNet architecture with compound scaling.....	21
Fig. 11. Hybrid EfficientNet-B5 and DOLG architecture.....	22
Fig. 12. Augmentation techniques used in our experiments.	24
Fig. 13. Sparse Categorical Cross Entropy.....	25
Fig. 14. Confusion matrix of (a) DenseNet and (b) Hybrid EfficientNet-DOLG on the COVID-19 classification task.	32
Fig. 15. Training history of (a) DenseNet and (b) Hybrid EfficientNet-DOLG on the COVID-19 classification task.	33
Fig. 16. Training and validation accuracy (a) loss (b) of DenseNet121.....	36
Fig. 17. Confusion matrix of (a) DenseNet and (b) Hybrid EfficientNet-DOLG on the COVID-19 severity assessment task	40
Fig. 18. Training history of (a) DenseNet and (b) Hybrid EfficientNet-DOLG on the COVID-19 severity assessment task.....	41
Fig. 19. Wide residual Networks architecture.....	42
Fig. 20. Visual Geometry Group Net architecture	43

Tables

Table 1. Detailed description of the COVID-19 classification dataset from the Chest X-Ray and COVIDX-CXR-3 datasets.	10
Table 2. Covid CT Scan images contribution from three datasets COVID-CT-Dataset, SARS-CoV-2, and COVID-CTSet.....	12
Table 3. Dataset contribution from RICORD and RALO dataset	14
Table 4. Detailed description of the six deep learning models used in thesis.	15
Table 5. Comparing results between the five deep learning models on the COVID-19 classification task with respect to precision metric score.....	29
Table 6. Comparing results between the five deep learning models on the COVID-19 classification task with respect to recall metric.....	30
Table 7. Comparing results between the five deep learning models on the COVID-19 classification task with respect to F1-score metric.....	31
Table 8. Classification results comparison of four deep learning models on CT Scan Images with respect to Precision metrics	34
Table 9. Classification results comparison of four deep learning models on CT Scan Images with respect to Recall metrics.....	35
Table 10. Classification results comparison of four deep learning models on CT Scan Images with respect to F1-score metrics	35
Table 11. Comparing results between the five deep learning models on COVID-19 severity assessment task with respect to precision metric.....	38
Table 12. Comparing results between the five deep learning models on the COVID-19 severity assessment task with respect to recall metric.	38
Table 13. Comparing results between the five deep learning models on the COVID-19 severity assessment task with respect to F1-score metric.	39

List of Abbreviations

AI	Artificial Intelligence
RT-PCR	Reverse Transcriptase–Polymerase Chain Reaction
RNA	Ribonucleic Acid
RSNA	Radiological Society of North America
RICORD	RSNA International COVID-19 Open Radiology Database
RALO	Radiographic Assessment of Lung Opacity Score Dataset
CXR	Chest X-ray
CNN	Convolutional Neural Network
WRNs	Wide Residual Neural Networks
VGG	Visual Geometry Group
CT Scan	Computed Tomography Scan
WHO	World Health Organization
LSTM	Long Short-Term Memory
LUNA16	Lung Nodule Analysis 2016
PMC	PubMed Central
DICOM	Digital Imaging and Communications in Medicine
TIFF	Tag Image File Format
CVPR	Conference on Computer Vision and Pattern Recognition
CIFAR	Canadian Institute for Advanced Research
GAN	Generative Adversarial Network
LDCT	Low-Dose Computed Tomography
NLP	Natural Language Processing

딥러닝을 사용한 흉부 X-선 및 CT 스캔을 통한 COVID-19 검출 및 심각도 등급 판별

Le Dinh Tuan

인공지능융합학과

요 약

COVID-19의 조기 식별은 신속한 의료 대응 계획과 치명적인 질병의 빠른 확산 속도를 늦추는 데 도움이 될 수 있다. COVID-19의 조기 선별 검사에서 RT-PCR을 대체하는 새롭고 혁신적이며 안전한 방법은 의료 영상 기법을 사용하여 COVID-19를 진단하는 것이다. 최근에 의료 영상 기술의 발전과 비전 알고리즘이 적용된 딥러닝의 성공으로 질병의 조기 진단을 위한 의료 영상 분석에 대한 연구가 많이 이루어지고 있다. 본 논문은 딥러닝을 사용한 흉부 X선 및 CT 스캔 사진 데이터 세트를 통한 COVID-19 검출 및 중증도 등급을 판별하는 방법을 제안한다. 특수 흉부 X선 및 CT 스캔 사진 데이터 세트에서 이러한 모델을 훈련(training)하기 전에 먼저 6가지 최첨단 딥러닝 기술에 대한 상세한 설명을 제공한다. 데이터 세트는 COVID-19 환자, 폐렴 환자 및 정상 상태의 사례로 구성하여 인공지능 시스템이 COVID-19를 검출하고 심각도를 결정하는 데 얼마나 잘 수행하는지 분석한다. 딥러닝을 사용한 COVID-19 조기 진단의 결과는 철저하고 안정적이며, 신뢰할 수 있는 전략으로 방사선 전문의에게 도움이 될 수 있음을 보여주었다.

COVID-19 Detection and Severity Grading with Chest X-Ray and CT-Scan Using Deep Learning

Le Dinh Tuan

Department of Artificial Intelligence Convergence,
the Graduate School,
Pukyong National University

Abstract

Early identification of COVID-19 may aid in both the planning of a prompt medical response and the slowing of the deadly disease's fast spread. One of the new, innovative, and safe methods to replace RT-PCR in the early screening of COVID-19 is to diagnose COVID-19 using medical imaging modalities. Recently, a lot of research has been done to analyze medical imaging for the early diagnosis of disease due to the improvement of medical imaging technology as well as the success of deep learning applied for vision tasks. The use of deep learning based on chest X-ray and CT scan to identify COVID-19 patients and severity grading is the subject of this thesis. We first offer a thorough explanation of six cutting-edge deep learning techniques before training these models on the specialized Chest X-ray and CT Scan picture dataset. The dataset comprises of COVID-19 cases, Pneumonia patients, and NORMAL instances to analyze how well artificial intelligence systems perform at detecting COVID-19 and determining its severity. The outcomes have demonstrated to us that deep learning may assist radiologists as a thorough, stable, and reliable strategy for early diagnosis of COVID-19.

I. Introduction

1.1 Coronavirus pandemic (COVID-19)

The COVID-19 coronavirus disease has been spreading and posing major threats to the lives and health of billions of people worldwide. Starting in Wuhan, China with the initial assumption caused by the animal selling in the local market, the novel Coronavirus has been rapidly expanding all over China and then spread to other countries. On January 30, 2020, the WHO (World Health Organization) announced the virus as an international concern at its highest emergency alert. The deadly virus can spread quickly and widely from one person to another through the air and surfaces of sick people, which is a crucial fact to be aware of.

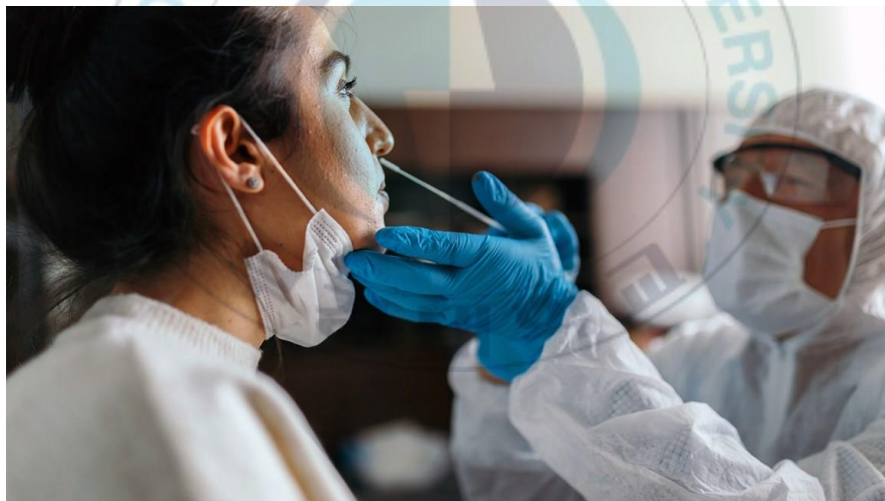


Fig. 1. Coronavirus PCR-RT Testing.

The main method to detect COVID-19 is the reverse transcriptase–polymerase chain reaction (RT–PCR) [1], which can detect axit ribonucleic SARS-CoV-2 (RNA) from the respiratory specimens (collected from nasopharyngeal swabs), is now the

gold standard for identifying COVID-19. However, RT-PCR has many limitations [2], and this screening method is a time-consuming procedure, laborious, complicated, and lacking supply devices. Some patients, including those highly suspected of COVID-19, have false negative and false positive results with the RT-PCR test, which indicates the poor sensitivity and highly variable results of the method [3] [4].

That is, to solve these problems globally, many attempts have been made to utilize available radiology medical imaging modalities to detect and analyze COVID-19. The two most popular types of images used for COVID-19 detection are Chest X-Ray and CT Scan images. Using medical images to detect new Coronavirus has gained many successes that prove the proper utilization of the method. However, the number of patients far exceeds the number of radiologists who take charge of diagnosing the input images. Thus, we need an automatic procedure to help these experts reduce the workload of classifying COVID-19 and NORMAL images.

1.2 Deep Learning for Medical Images Analysis

Despite Chest X-Ray and CT Scan diagnosis having many advantages, it still faces some obstacles due to some idiosyncratic characteristics of the new pandemic disease. The most cumbersome obstacle is the lack of experienced radiologists and also the error-prone human visual indicators. Computer aid design diagnosis can help radiologists to have faster and more accurate COVID-19 diagnosis as a crucial adjunct to reduce workload and enhance patient safety [5] [6].

Recently, with the emergence of deep learning, many studies have been conducted to analyze the potential of Deep Learning for Medical Image Analysis [7] [8], especially to apply deep learning for automatic COVID-19 detection [9] [10]. Deep learning for COVID-19 detection could help solve the problem of a lack of radiology specialists and also produce reliable performance [11] [12]. However,

almost all developed artificial intelligence (AI) systems are not open and are not available for the research community to access resources. We do not have much open-source coding or datasets available to conduct thorough research on the subject. Recently, there have been significant efforts pushing for access to the resource and AI source code about detecting COVID-19 using Chest X-Ray images; some of the notable research can be found in [13] [14]. In one study, a tailored convolution neural COVID-NET [15] architecture was created to classify normal, pneumonia, and COVID-19. Different from other studies, the author of this study used a large dataset containing 13,800 Chest X-Ray images on 13,645 patients. The authors gained accuracy results of 92.4% with COVID-19 classification performance.

Severity Grading using Chest X-Ray is not an easy task, even with experienced radiologists; clinical diagnosis with the aid of a computer could help doctors with this daunting task. There are some works related to COVID-19 severity grading [16] [17], including the deep learning applied works of Liang et al. [18] and COVID-Gram [19] in which the author investigated the X-Ray abnormality to detect COVID-19. In the work of Colombi et al. [20], the lung pneumonia extent was diagnosed to assess the severity of the disease. Another notable work was COVID-NET-S [21], one of the early COVID-19 severity grading studies in which the author designed a deep neural network to predict extent scores from Chest X-Ray images.

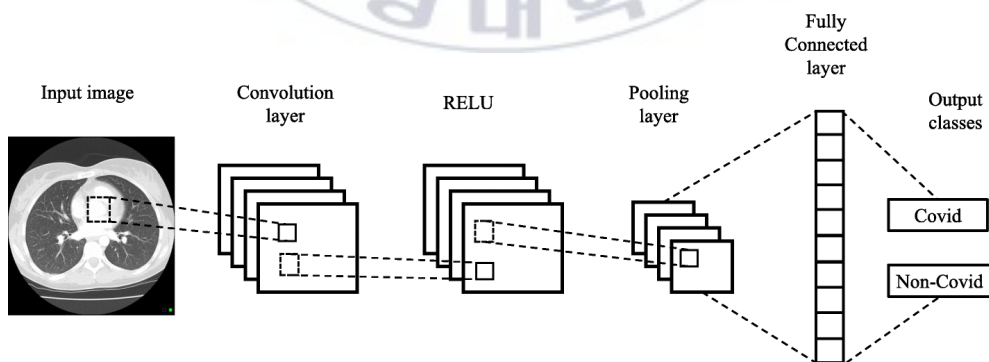


Fig. 2. Apply Deep Learning for Medical Image Classification.

1.3 Outline of Thesis

In this thesis, we study the application of deep learning for detecting COVID-19 based on Chest X-Ray and CT Scan images. The experimental results have shown us that artificial intelligence methods based on deep neural networks could aid doctors and radiologists with high accuracy and reliable performance. Furthermore, we also study the assessment of COVID-19 severity through classified Chest X-Ray images. The patient severity is divided into level1 and level2, which indicates the seriousness of the illness and can aid doctors in deciding a treatment response. We collected training images from various open dataset sources and then cleaned the input data by removing low-quality images and separating the original dataset to balance sets for efficient training. We trained six deep learning models on the customized datasets and evaluated model performance on three metrics: precision, recall, and F1-score.

The rest of this thesis is organized as follows. Section II discusses related works about COVID-19 detection and severity grading. Section III describes the customized datasets used for the experiment and goes into more detail about deep learning architectures to train these datasets; we also explain preprocessing and some settings for the training pipeline; five evaluation metrics are presented and each formula is discussed. At the end of the thesis, we recap our study and address some future works to enhance our experiment results.

II. Related Works

2.1 COVID-19 Detection Using Chest X-Ray

One of the recent emerging screening methods for COVID-19 is thoracic imaging analysis, which can be applied in early COVID-19 detection [22] [23]. These Chest X-Ray images are obtained and analyzed by radiologists to find visual indicators related to SARS-CoV-2 viral infection. Former studies prove that COVID-19 causes abnormal areas that could be visible in Chest X-Rays;

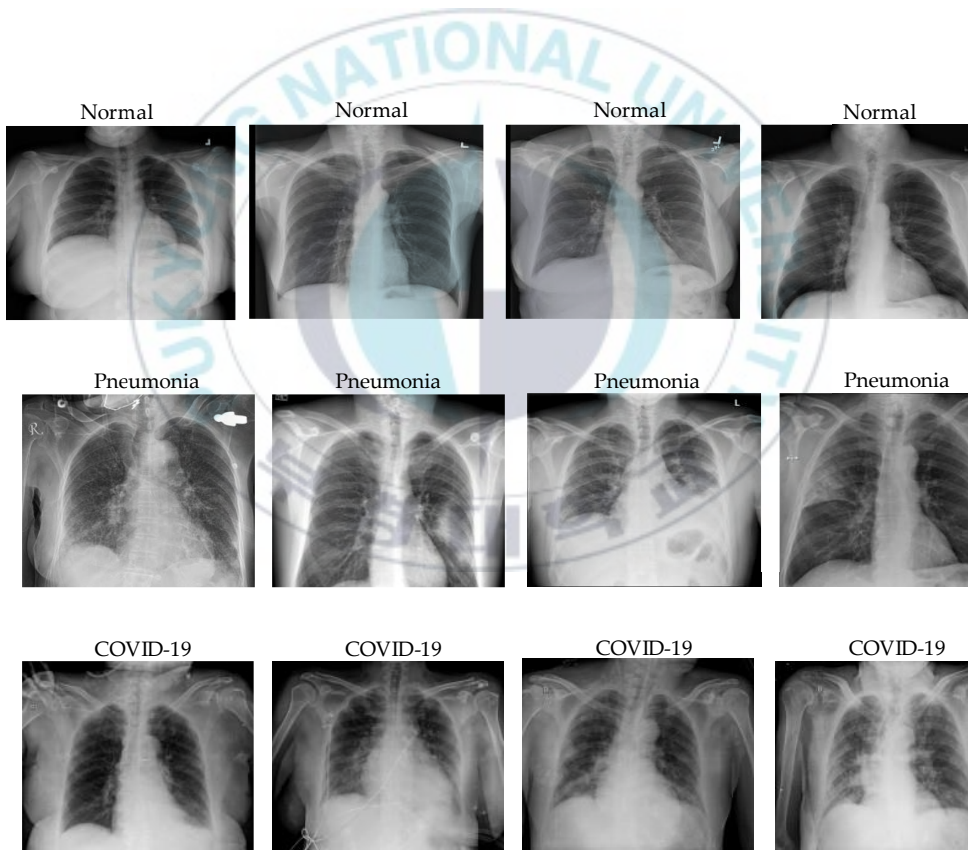


Fig. 3. Chest X-Ray for COVID-19 Detection.

This hypothesis could be a strong suggestion to use Chest X-Rays as the initial step for COVID-19 monitoring [24] [25]. Some of the most cutting-edge benefits when using Chest X-Rays for COVID-19 diagnosis include the following:

- Chest X-Ray diagnosis allows us to have rapid COVID-19 classification and could be carried out in parallel with RT-PCR testing to deal with high volumes of patients.
- Chest X-Ray images could be obtained in many clinical sites and are readily available in most health care centers.
- The portable Chest X-Ray imaging system helps doctors to isolate the image capturing process from other people such that it can reduce the risk of spreading COVID-19.

2.2 COVID-19 Detection Using CT-Scan

Deep Learning methods applied for radiology had seen a very successful scheme. Many notable works have been done for the detection of COVID based on X-Ray images, especially for CT Scan images. In the work of Anthony Ortiz et al. [26] the authors had developed an architecture which calculates the total volume of chest CT then represents in 2D data for simple integration with clinical data to detect COVID-19 from CT Scan images. Another work of Ahmed Mohammed et al. [27] proposed a weakly-supervised deep learning architecture based on ResNext and Long Short Term (LSTM) to detect COVID-19 with very few labeled input data.

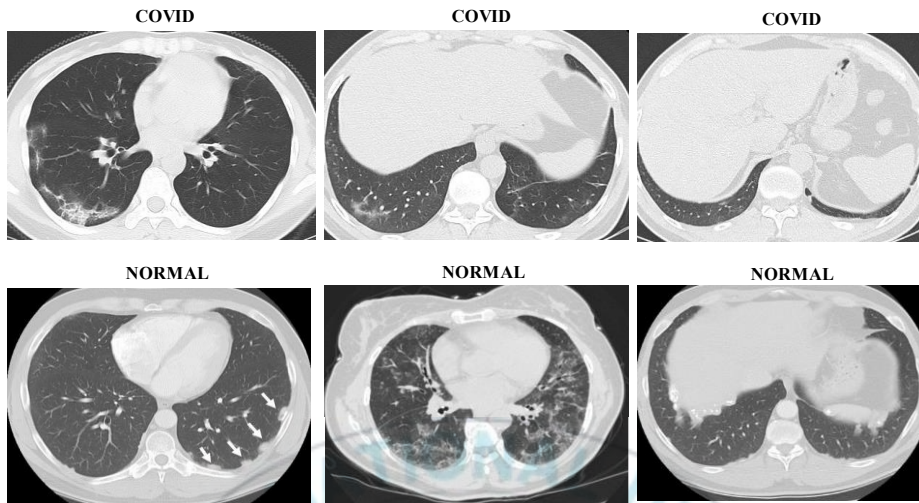


Fig. 4. CT Scan Images apply for COVID-19 Detection.

Tahereh Javaheri et al. [28] created CovidCTNet which is an open-source collection of deep learning methods which facilitate doctors, radiologists, physicians on the screening process of COVID-19 detection. Parnian Afshar et al. [29] proposed a capsule network that can reach human-level in COVID-19 detection performance on low-dose and ultra-dose CT Scan images. The architecture uses a two-stage capsule network and run experiment on a collection of LDCT/ULDCT dataset which reduces the radiation exposure and still remain the image resolution. Edward H. Lee et al. [30] designed Deep COVID DeteCT which used to detect COVID-19 on CT images, which consists of 27 feature extractor layers of 3D Inception, 3D average pooling, and one fully connected layer. The experiment had conducted on a large and diverse population across 13 international organizations and 8 countries.

2.3 COVID-19 Severity Grading Using Chest X-Ray

Various Deep Learning models were created to assist COVID-19 detection based on Chest X-Ray images [15] [31]. With the rapid emergence of AI models, still have

some limitations due to the weakness of methodology and biases [32]. First, the publicly Chest X-Ray dataset often has varied quality and lack of validity. We need to have high-resolution images and multi-center image sources to have a more effective baseline. Second, we need to have a balanced dataset that has equal numbers of positive as well as negatives cases to have a more generalized machine learning model, however, due to the rapid change of COVID-19 in the community and the sensitivity of the deep learning model with the unbalanced dataset, the generalization of COVID-19 model is not yet understood.

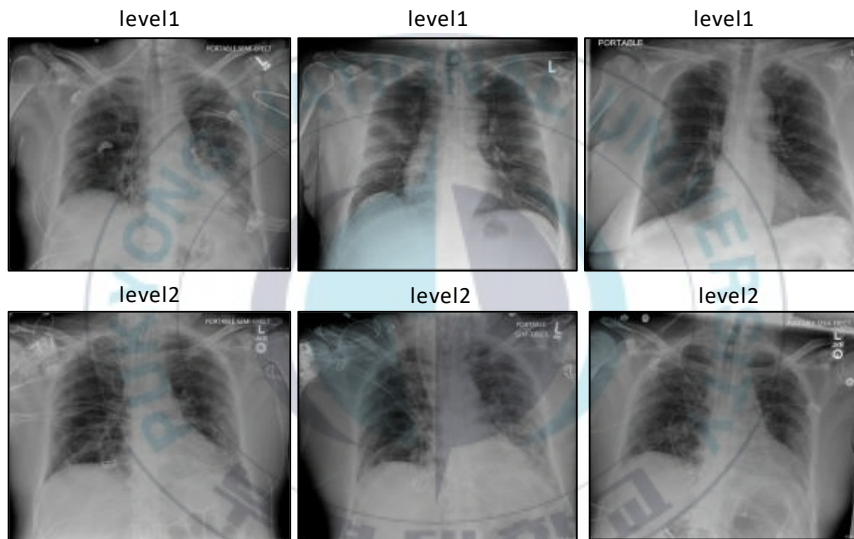


Fig. 5. COVID-19 Severity Assessment Using Chest X-Ray Images.

The use of deep learning in processing and analyzing medical images is a challenging field of AI [33]. In the work of [34] the authors used a special deep learning model called SqueezeNet because it has a smaller structure compared to other famous neural nets. The main focus of this new architecture is to obtain higher accuracy so the optimization of parameters is a priority task [35].

While most of the research material focuses on the detection of COVID-19 with the aid of a computer using Chest X-Ray images, the work of assessing COVID-19

severity is not well explored. Some notable works in this field are COVID-Net S, a tailored convolution neural network designed by Wong et al. [36] and the work of Cohen et al. [37] which tries to gauge the severity of COVID-19 for the treatment response of serious cases.



III. The Proposed Methods and Results

3.1 Dataset

3.1.1 COVID-19 Detection Chest X-Ray Dataset

We collected the COVID-19 classification dataset from two open datasets. The first is COVID CXR dataset which contains 30,128 images in total. There are 16,488 images labeled as COVID-19 and 5555 images labeled as pneumonia and 8085 images labeled as normal. The whole dataset was collected from five open-source datasets which are currently freely available. The second dataset is the Chest X-Ray Images (Pneumonia) dataset which was published on the Kaggle competition to classify pneumonia and normal Chest X-Ray images. We mixed the two datasets together and removed portions of COVID-19 labeled images from the COVID CXR dataset to create a more balanced dataset. Details about the dataset contribution are illustrated in Table 1, in which the COVID CXR was collected from 5 published datasets which account for 80% of the mixed dataset. We made the combined dataset cleaner by removing all low-quality images and keeping the high-quality images only, then data augmentation was used to feed images into the deep learning models.

Table 1. Detailed description of the COVID-19 classification dataset from the Chest X-Ray and COVIDX-CXR-3 datasets.

Sets	Category	Chest X-Ray	COVIDX-CXR-3	Total
Train	COVID-19	-	13,192	13,192
	Normal	3290	4444	7734
	Pneumonia	3418	4444	7862
Validation	COVID-19	-	3298	3298

	Normal	821	1111	1932
	Pneumonia	855	1111	1966
Test	COVID-19	-	200	200
	Normal	-	100	100
	Pneumonia	-	100	100

The Chest X-Ray Pneumonia dataset contains a total of 5856 images which are grouped into two categories, normal and pneumonia. There are 1583 images labeled as normal and 4273 images labeled as pneumonia. All the normal and pneumonia images were then mixed with normal and pneumonia images from the COVID CXR dataset.

The total number of COVID-19 images is 9446, normal is 9668, and pneumonia is 9828. The Chest X-Ray images were selected from Guangzhou Women and Children’s Medical Center, Guangzhou. All those images were collected as the clinical checking routine for patients suffering from pneumonia. The Chest X-Ray images were cleaned to make sure the quality of the input images was acceptable to feed into deep neural models. These images were classified by two expert radiologists and double-checked by a third radiologist.

3.1.2 COVID-19 Detection CT Scan Dataset

Three open-source datasets were used to collect data for the training pipeline. We take images from the COVID-CT-Dataset [38], SARS-CoV-2 [39], and COVID-CTSet [40], with a proper image number to have a balanced dataset between categories. The dataset contribution was summarized in Table 2 with a detailed number of images taken from each dataset.

COVID-CT-Dataset: The Dataset contains 349 COVID-19 CT images from 216 patients and 463 NORMAL CT images. The labeling process was done by a radiologist expert who has been in charge of treating those patients since Coronavirus pandemic outbreaks. All 760 COVID-19 images were collected from medRxiv and bioRxiv with the associated metadata. Firstly, the author manually selected CT images, then read all the captions to judge whether positive for COVID. In case the judgment cannot be made, the author will analyze the text from preprint documents to make a decision. For the NORMAL CT Scan images, the author utilized datasets from many sources, including MedPix, LUNA16, Radiopaedia website, and PubMed Central (PMC). The MedPix is an online open-source medical image database, that aims to provide rich medical data for medical, nurses, students, physicians, and health professionals. The LUNA16 dataset published in the scope of Lung Nodule Analysis 2016, which captured from 888 scans and labeled by four experienced radiologists. Radiopaedia website is an open website with the purpose to provide publicity and free data about medical images the same as Wikipedia. There are thousands of patient cases published on the website and we can access them freely. PubMed Central (PMC) is a large research database storing academic journal papers related to biomedical and life science.

Table 2. Covid CT Scan images contribution from three datasets COVID-CT-Dataset, SARS-CoV-2, and COVID-CTSet

Dataset	Train		Test	
	<i>COVID</i>	<i>NORMAL</i>	<i>COVID</i>	<i>NORMAL</i>
COVID-CT-Dataset	280	318	69	79
SARS-CoV-2	1002	983	250	246
COVID-CTSet	1820	1916	462	462

SARS-CoV-2: The dataset contains 1252 COVID and 1230 NORMAL CT scan images which include a total of 2482 images. These images were captured from hospitals around Sao Paulo, Brazil with the purpose to encourage the study of finding an artificial intelligence technique to detect COVID-19 from CT scan images. There are 60 patients diagnosed with COVID-19, of which there are 32 males and 28 females in this group. There are 60 patients who do not infect with COVID-19, and there was a total of 30 males and 30 females. To evaluate the performance of this dataset, the author had run experiments on different deep learning models. The proposed xCNN model produced the best result when training on the SARS-CoV-2 dataset with the explainable deep learning approach. The method had gained 97,31% as an F1 score metric and could provide a new quick, safe and reliable technique for the COVID-19 detection method.

COVID-CTSet: The dataset was captured from Negin radiology in Sari, Iran between the period from 5th March to 23rd 2020. There are total of 48, 260 chest CT Scan images captured from 282 COVID-19 patients and 15, 589 images of 282 normal people. The Negin radiology had used the SOMATON scope model to capture 16-bit grayscale DICOM images with 512 x 512 resolution. The author uses 16-bit grayscale images instead of 8-bit since converting the original DICOM 16-bit to 8-bit might lose important information. Moreover, the 16-bit DICOM might contain information that human eyes cannot see, but the computer could process this information that helps the deep learning model enhance the classification performance of deep learning models. Because the patient's information could retrieve from DICOM images, the author had converted original images from DICOM to TIFF format. These converted images have the same 16-bit grayscale in color, however, do not contain any patient information. In addition, the TIFF image format is easy to read and processed by the popular image processing library. For precise model training output, a clinical expert labeled input images and a third radiologist expert supervised all COVID-19 CT images to exactly classify input data.

3.1.3 COVID-19 Severity Grading Dataset

We collected covid severity images using two open-source datasets: RICORD and RALO. The datasets contain images from two categories level1 and level2, which denoted the severity status of patients. If patients were diagnosed as level1, they could self-quarantine at home and no need to have further treatment support and if patients were diagnosed as level2 they should go to the hospital and need assistance from doctors. We mixed two dataset images together and removed all low-quality images, kept the high-quality ones then separated them into training, validation, and test sets.

RICORD dataset: The RICORD dataset shorts for the RSNA International COVID-19 Open Radiology Database which is a multi-institutional, multi-national coronavirus imaging dataset. The RICORD dataset is collected from 4 countries which represent the diversity of the COVID-19 case all around the world. The images were labeled by experienced volunteer radiologists with the aim to have a more precise diagnosis and assessment for the severity of the COVID-19 cases. These radiologists have spent hundred hours collecting, organizing, and labeling the dataset with an effortless contribution. The RICORD dataset contains 240 CT scan images and 1000 Chest X-Ray images, including the meta-information about age, sex, status, and the COVID-19 testing methods.

Table 3. Dataset contribution from RICORD and RALO dataset

Sets	Category	RICORD	RALO	Total
Train	level1	140	845	985
	level2	467	1054	1521
Validation	level1	35	211	246
	level2	117	263	380

Test	level1	52	-	52
	level2	98	-	98

RALO dataset: The RALO dataset contains 2373 Chest X-Ray images and was captured from Stony Brook Medicine. Each image was scored by two radiologists with the score including Right Geographic, Right Opacity, Left Geographic, Left Opacity, and total Opacity. Both the dataset was published as freely available with the purpose of research and education only, without commerce.

3.2 Deep Learning Architectures

We used five neural networks to conduct our experiment, three convolutional, and two transformer-based models. The overview of each model architecture is shown in Table 4 and the details are presented in the following sections.

Table 4. Detailed description of the six deep learning models used in thesis.

Architecture	Input Shape	Trainable Parameters	Non-Trainable Parameters	Total Parameters
DenseNet121	(384, 384, 3)	6,956,931	83,648	7,040,579
ResNet50	(384, 384, 3)	25,583,592	53,120	25,636,712
InceptionNet	(384, 384, 3)	54,673,507	63,616	54,737,123
Swin Transformer	(224, 224, 3)	86,746,299	336,140	87,082,439
EfficientNet	(384, 384, 3)	18,454,835	170,574	18,625,530
Hybrid EfficientNet-DOLG	(384, 384, 3)	32,843,059	170,695	33,013,754

3.2.1 DenseNet121

The DenseNet121 [41] model won the CVPR 2017 Best Paper Award and was invented by researchers from Cornell University, Tsinghua University, and Facebook Research. The convolution neural net contains shorter connections between input and output layers so that the network can be deeper, more efficient, and more accurate. Based on these observations, Gao Huang et al. introduced DenseNet, which connects each layer following the deep-forward design principle. With each layer, a feature map of all layers is used as the input and its own feature map is then used for the next layers. The DenseNet architecture has many strong points: it reduces the gradient descent, enhances features propagation, promotes features reuse, and reduces a large number of parameters.

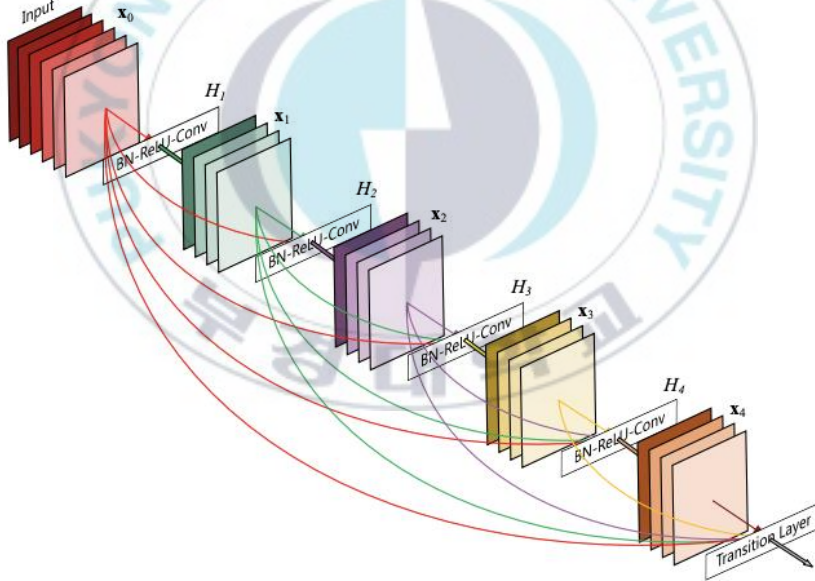


Fig. 6. DenseNet121 overall architecture

We have a convolutional neural network (CNN) with L layers, an image x_0 passing through the network. We denote subscript l as the l^{th} layer, $H_l(\cdot)$ is a

nonlinear transformation, and output of l^{th} layer is x_l . In the conventional CNN, the output of l^{th} layer is given as:

$$x_l = H_l(x_{l-1})$$

In ResNet, a new skip connection technique is proposed to tackle gradient vanishing problem, the output of $l - 1^{th}$ layer is added with the identity function:

$$x_l = H_l(x_{l-1}) + (x_{l-1})$$

Instead of simple summation of identity function and the output of $H_l(\cdot)$, DenseNet proposed the dense connectivity which take the input from concatenation of previous layers:

$$x_l = H_l([x_0, x_0, \dots, x_{l-1}])$$

In which, $[x_0, x_0, \dots, x_{l-1}]$ is concatenation of x_0, x_0, \dots, x_{l-1} layers.

3.2.2 ResNet50

ResNet architecture was proposed by Kaiming He et al. [42] to solve the problem when training very deep neural networks. Prior convolutional neural networks often face the issue of gradient vanishing when a large number of layers are stacked into the neural network. Gradient vanishing appears when the network is too deep, and the gradient calculated from the loss function easily decreases to zero through several chain rule operations. This results in the model not learning anything from the training process as there is no weight updating.

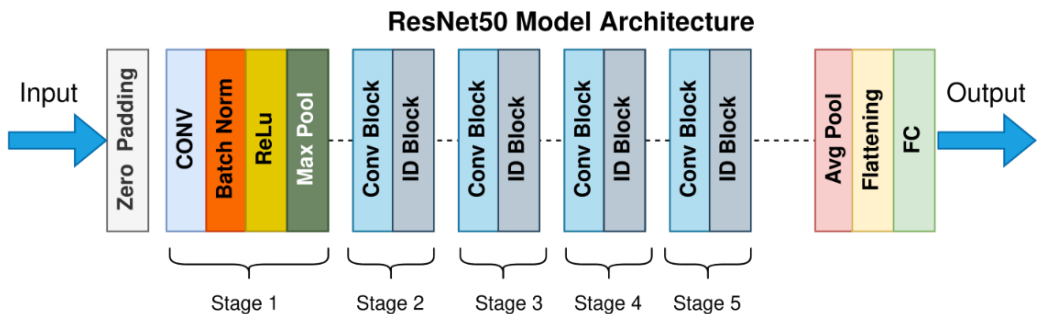


Fig. 7. ResNet50 Model Architecture

The main concept of ResNet is the skip connection mechanism which reduces the gradient vanishing in two ways. First, it establishes a shortcut for the gradient passing through many layers, which helps the gradient to still pass over many layers. Second, it allows the model to learn an identity function which makes sure that the higher layers do not perform worse than the lower. In this paper, we use ResNet50, which is a variant of ResNet and has 50 layers, including 48 convolution layers and 1 max-pooling, and 1 average pool layer.

ResNet adopt residual learning mechanism, we have x and y are the input and output of the l^{th} layer, consider the building block:

$$y = F(x, \{W_i\}) + x$$

In which, function $F(x, \{W_i\})$ denotes the residual mapping to be learned. The summation operation: $F + x$ represents the shortcut or the skip connection element-wise operation.

3.2.3 InceptionNet

Before InceptionNet, prior convolutional neural networks mainly focused on increasing the depth of the network to extract features for improving the learning ability of the model. However, the creators of InceptionNet [43] pioneered the scaling of both depth and width of the model while still maintaining constant hardware usage. The principal idea behind the InceptionNet model is that every neuron which extracts the same features should learn together. Furthermore, InceptionNet architecture focuses on parallel processing and extracting different feature maps simultaneously.

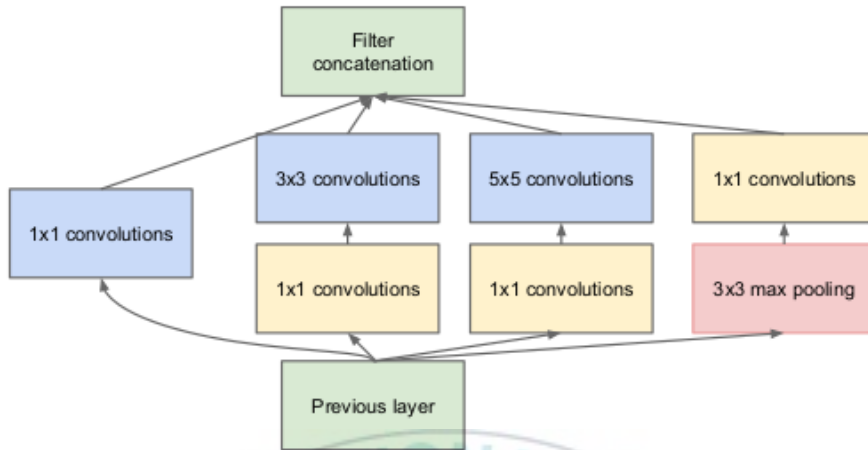


Fig. 8. InceptionNet module with dimensionality reduction

This is the key innovative aspect that makes InceptionNet unique from other convolutional neural networks before it. However, InceptionNet architecture also has some disadvantages, for example, large models which use InceptionNet are subjected to overfit, especially with limited numbers of labeling input data. The model will bias toward the category which has more labels than another category.

3.2.4 Swin Transformer

Winning the Best Paper Awards and Best Student Paper competition, the Swin Transformer [44] is listed on the priority choices to run our experiments. The model had solved many problems that many vision transformers before it experienced, and it also makes a significant shift in applying transformer for vision tasks. We face a substantial challenge when applying transformer from natural language processing to computer vision, because of the natural difference between these two tasks, for example, a large number of pixels in high-resolution images far exceeds the number of words in text documents.

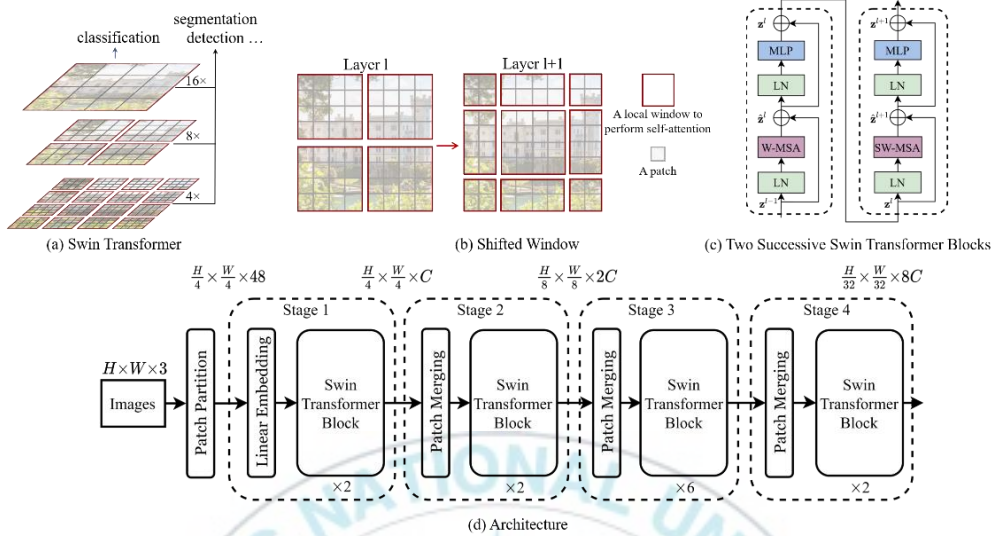


Fig. 9. Swin Transformer with Shifted Window Architecture

Which makes the transformer for vision tasks cost more expensive computationally than applying transformer for NLP. In order to solve this problem, the creators of Swin Transformer proposed a hierarchical architecture of transformer which has representation computed by shifted windows. This hierarchy provided a flexible ability to model at different scales and has linear complexity with image size. Therefore, it can be used as the backbone for other vision tasks such as classification and dense prediction.

3.2.5 EfficientNet

EfficientNet was proposed by Mixing Tan and Quoc Le [45], in their work, the authors studied the relationship between the depth and the wide of the model compare with the network performance of the network. They concluded that if we apply to scale on both the depth, the wide, and the resolution of input images, we get a new type of model that has fewer parameter numbers and has better classification performance. These categories of model architecture called EfficientNet ranging from B0 to B7 and had passed all prior state-of-the-art models on the classification

task of ImageNet Challenge. The main building block of EfficientNet is the MBCConv (Mobile ConvNets) which have origin in MobileNet architecture [46]. Compare to other convolutional neural networks such as ResNet50 [47] with a total of approximately 20 million parameters and the EfficientNet B0 with only 5 million parameters the EfficientNet model still performs a better classification accuracy.

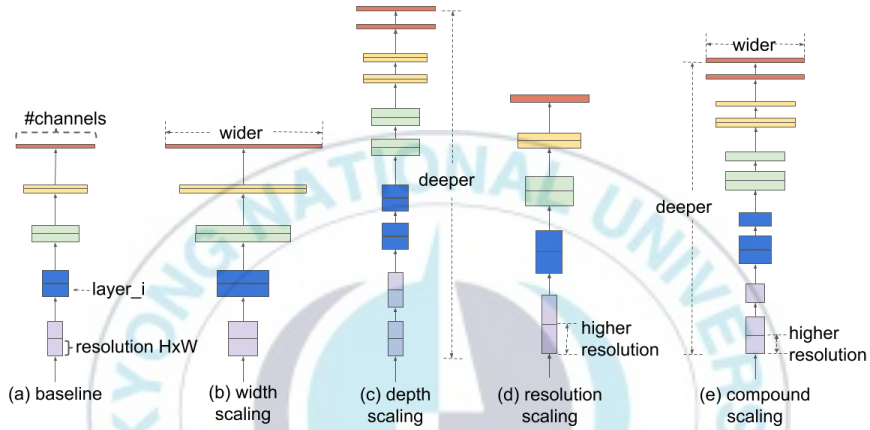


Fig. 10. EfficientNet architecture with compound scaling

The important contribution of the EfficientNet is the new compound scaling method, that uniformly scales the network in terms of depth, width, and resolution of input images. The scaling method is demonstrated in the following principle:

$$\begin{cases} \text{depth: } d = \alpha^\Phi \\ \text{width: } w = \beta^\Phi \\ \text{resolution: } r = \gamma^\Phi \end{cases}, \quad s.t. \alpha \cdot \beta^\Phi \cdot \alpha^\Phi \cdot \gamma^\Phi \approx 2, \alpha \geq 1, \beta \geq 1, \gamma \geq 1$$

In which, α, β, γ are constant coefficients which can be calculated by a small grid search on the original small model. And Φ is coefficient predefined by users

that control resources for model scaling. If we scale the network depth α^N , width β^N , and resolution γ^N then we get 2^N times more computational resources.

3.2.6 Hybrid EfficientNet and DOLG

The Hybrid EfficientNet and DOLG [48] won the Google Landmark Competition 2021 with the highest recognition performance on the over 200,000 classes. The author implemented the model by enhancing the original DOLG [49] with some adjustments to improve the recognition capability. At first, the author used the EfficientNet [45] which was pre-trained on the ImageNet dataset as an encoder. Then the author added a local branch after the third EfficientNet block and extracted those 1024 dimensions of local features by using three dilated convolutions where parameters were different per each model.

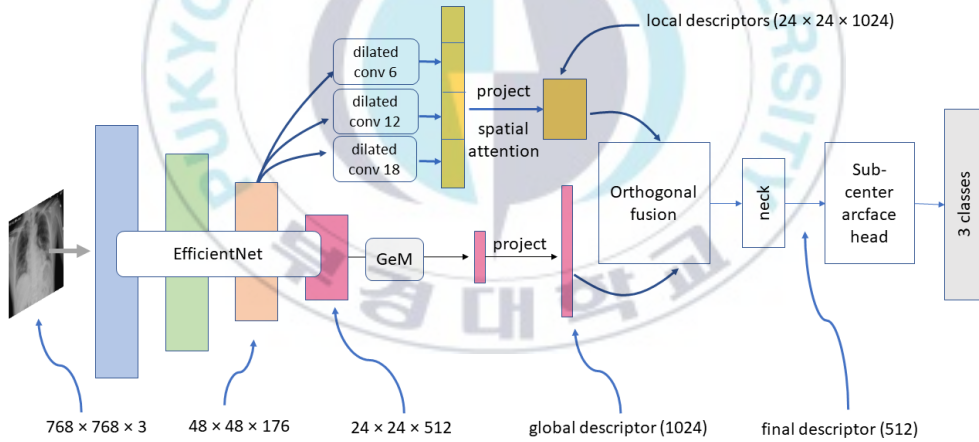


Fig. 11. Hybrid EfficientNet-B5 and DOLG architecture.

The output of the fourth EfficientNet was projected to 1024 dimensions and those fused features accumulate using the average pooling before they were fed into the fully connected layers. The model used the subcenter arc face as the loss function contains dynamic margins for predicting thousands of classes. Overview architecture

of Hybrid EfficientNet and DOLG illustrates in Figure 3 with EfficientNet-B5 as a feature extractor and DOLG as a classifier.

3.3 Preprocessing and Training Setting

3.3.1 Data Augmentation

Recently, convolutional neural network and transformer performed excellently on many vision tasks such as classification and segmentation. However, these networks need more input data to prevent overfitting, which leads to the failure of the model generalization. These models overfit when learned weights are performed well on the training set, however, badly on the testing set. Unfortunately, many application domains of deep learning do not have access to big data, such as the medical and biomedical domains, in which input data are scarce because of the costly labeling expense and the scarcity of image sources. We need to have experienced radiologists, pathologists, and specialists in medical images analysis to perform labeling of input data which makes the cost of labeling data become too expensive. Furthermore, many real-life medical data cannot be available for the privacy protection of patient information.

One of the common techniques usually used to increase input image data for deep learning models is to apply data augmentation operations. Many works apply deep learning for COVID-19 detection using Chest X-Ray data augmentation techniques to increase input data. In the work of COVID-NET, Wang et al. [15] applied horizontal flip, intensity shift, translations, zoom, and rotation. The work of Bassi et al. [50] applied flipping, rotations, and translation methods to improve the deep neural network performance. Another work by Nishio et al. [51] used a mixture of data augmentation techniques, such as rotating, flipping, shifting, and mix-up to improve the model's performance. In this paper, we utilized various image transformation techniques using *ImageDataGenerator* from

keras.preprocessing.image to augment our input data. Image augmentation operations include *height_shift_range*, *rotation_range*, *horizontal_flip*, *brightness_range*, *width_shift_range*, and *rescale*.

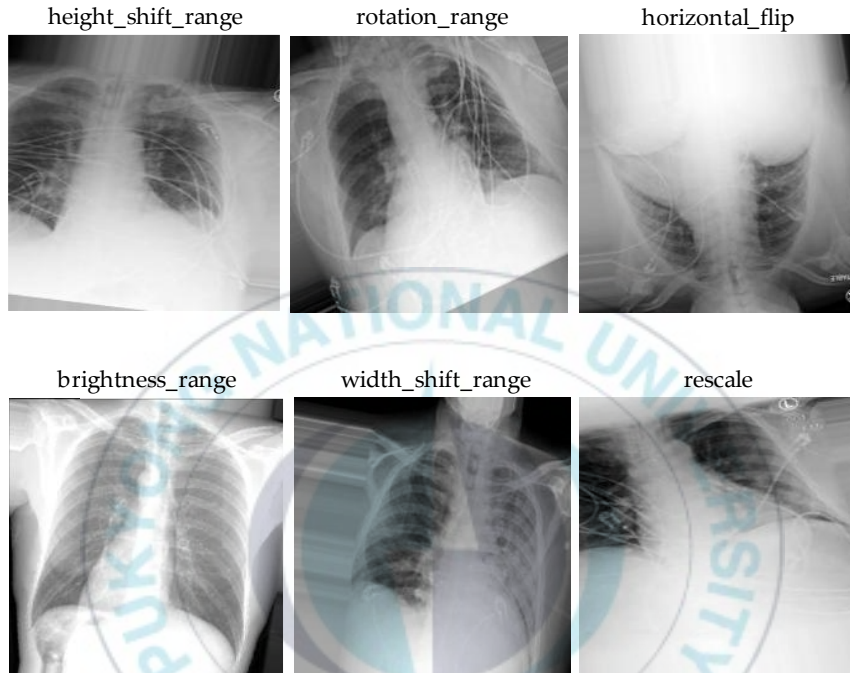


Fig. 12. Augmentation techniques used in our experiments.

3.3.2 Hardware and Hyperparameter Setting

We trained deep learning models on the NVIDIA GeForce RTX 2070 GPU 8GB with the computer hardware setting: Intel(R) Core (TM) i7-8700K CPU @ 3.70GHz RAM 16GB. We used *CallBack*, *ModelCheckpoint*, *LearningRateScheduler*, *TensorBoard*, *EarlyStopping*, and *ReduceLROnPlateau* from *tensorflow.keras.callbacks*. We set the maximum epoch to 120 with a patience of 10, starting with a learning rate to 0.0001 with a minimum learning rate of 0.0001 and maximum learning rate of 0.0005. We utilized the Adam optimizer [52] from

tensorflow_addons, which is the upgrade version of the stochastic gradient descent and has been used frequently for vision and natural language processing.

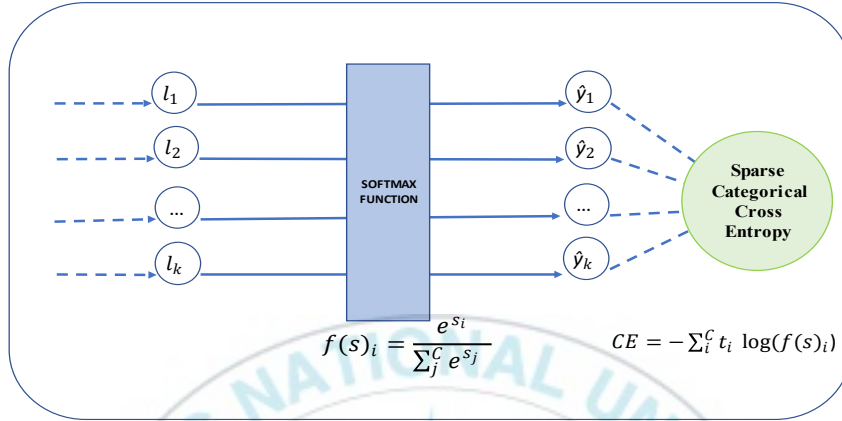


Fig. 13. Sparse Categorical Cross Entropy

We used Sparse Categorical Cross Entropy as the loss function for our training pipeline, which is a loss function applied for multi-categorical classification. There are two loss functions usually applied for the multi-categorical classification tasks, which are categorical cross entropy and sparse categorical cross entropy. The two loss functions have the same formula as illustrated in the diagram above; however, the only difference is the truth value in sparse categorical cross entropy, which are integer encoded such as {1}, {2}, {3}, and the categorical cross entropy use of one-hot encoding, such as {1, 0, 0}, {0, 1, 0}, and {1, 0, 1} instead. Illustration of multi-categorical classification scheme presents in Figure 5 with feature maps goes through Softmax layer before passing to Sparse Categorical Cross Entropy.

3.4 Evaluation Metrics

In our experiment, we used evaluation metrics from *classification_report* in *sklean.metrics* which include precision, recall, F1-score metrics with respect to each

category, macro average and micro average. Details about metrics are presented in the following sections.

3.4.1 Precision Metric

$$\textit{Precision} = \frac{\textit{True Positive}}{\textit{True Positive} + \textit{False Positive}}$$

The precision metric calculates the ratio between positive observations which was predicted correctly and the total positive observations. Precision is a good metric to evaluate our machine learning models when the cost of false positives is high.

3.4.2 Recall Metric

$$\textit{Recall} = \frac{\textit{True Positive}}{\textit{True Positive} + \textit{False Negative}}$$

The recall metric calculates the ratio between positive observations which was predicted correctly and the total actual positive observations. Recall actually calculate the number of actual positive that our model predicts via labeling it as true positive. Recall metric might be used when there is a high cost of false negatives.

3.4.3 F1-score Metric

$$\textit{F1 - Score} = 2 * \frac{\textit{Precision} * \textit{Recall}}{\textit{Precision} + \textit{Recall}}$$

F1-score metric calculated by using the precision and recall of the models then taking the harmonic mean of them. This metric is mainly used to compare performances of two machine learning models. For example, if model A produces better precision but model B produces higher recall then for this case, we should use F1-score to choose the best model.

3.4.4 Macro-Average Metric

When dealing with multi-categories task, to find the average metric of all these categories, we have two kinds of metrics, which are Macro Avg and Micro Avg. The difference between Macro Avg and Micro Avg is that the Macro Avg compute precision, recall, and f1-score for each category individually and then takes the average of them. In contrast, Micro Avg take the calculation of the lower components like true positives, false positives, true negative, and false negative to compute the average.

$$\text{MacroAvgPrecision} = \frac{P1 + P2}{2}$$

$$\text{MacroAvgRecall} = \frac{R1 + R2}{2}$$

$$\text{MacroAvgF1 - score} = \frac{F1 + F2}{2}$$

For example, when computing Macro avg of precision, we have two classes: class 1 and class 2, with P1 is the precision metric of class 1 and P2 is the precision metric of class 2. We then calculate the average of P1 and P2, which is then compute the mean of P1 and P2

3.4.5 Macro-Average Metric

Similar to Macro Avg, the second average metric Micro Avg also computes the average performance of all categories based on precision, recall, and f1-score. The difference is that Micro Avg determines this metric by executing the calculation of numbers like true positives, true negatives, false positives, false negatives, MicroAvgPrecision, and MicroAvgRecall:

$$\text{MicroAvgPrecision} = \frac{TP1 + TP2}{TP1 + TP2 + FP1 + FP2}$$

$$\text{MicroAvgRecall} = \frac{TP1 + TP2}{TP1 + TP2 + FN1 + FN2}$$

$$\text{MicroAvgF1 - score} = \frac{\text{MicroAvgPrecision} * \text{MicroAvgRecall}}{\text{MicroAvgPrecision} + \text{MicroAvgRecall}}$$

For example, to compute MicroAvgF1-score we will take the harmonic mean of MicroAvgPrecision and MicroAvgRecall.

3.5 Results and Discussion

We ran experiments on two tasks. The first task included normal, pneumonia, and COVID-19 classification, which was a multiple-categorical classification task. The second task was the COVID-19 severity assessment, which included two levels of severity and turned out to be a binary classification task

3.5.1 COVID-19 Chest X-Ray Classification Results

We trained three convolution-based and two transformer-based models on the customized COVID-19 classification dataset. The output results were evaluated based on three metrics, which were precision, recall, and F1-score with respect to COVID-19, normal, pneumonia, macro-average, and micro-average. Each tables below contained numerical results of three metrics and will be described in detail. The two models which showed the best results were DenseNet121 and Hybrid EfficientNet-DOLG.

Table 5. Comparing results between the five deep learning models on the COVID-19 classification task with respect to precision metric score.

Methods	Precision				
	COVID-19	Normal	Pneumonia	Macro-Average	Micro-Average
DenseNet121	0.98	0.91	0.94	0.94	0.95
ResNet50	0.98	0.83	0.93	0.92	0.94
InceptionNet	0.98	0.83	0.90	0.90	0.92
Swin Transformer	0.99	0.62	0.89	0.83	0.87
Hybrid EfficientNet-DOLG	0.98	0.93	0.93	0.95	0.96

Table 5 compares the performance of five deep learning models based on the precision metric score. The numerical results illustrate each category and on macro- and micro-average. For the COVID-19 precision score, the best model was found to be Swin Transformer with a score of 0.99, and for normal images, we found Hybrid EfficientNet-DOLG a top score of 0.93, and for pneumonia, the DenseNet121 model produced the highest result (0.94). For macro-average and micro-average, the Hybrid EfficientNet-DOLG was found to lead both metrics with scores of 0.95 and 0.96, respectively. The hierarchical architecture of Swin Transformer computed image representation in different scales which works best on COVID-19. On the other hand, the concatenate mechanism of DenseNet boosted the pneumonia detection of DenseNet. The hybrid architecture helped Hybrid EfficientNet-DOLG perform best results on normal, macro average, and micro average.

As shown in Table 6, we could see the outstanding performance of Hybrid EfficientNet-DOLG as it produced the highest score on three metrics: pneumonia,

macro-average, and micro-average, with scores of 0.95, 0.96, and 0.96, respectively. For the COVID-19 category, we found the DenseNet121 to have a recall score of 0.98 and the second highest score was found to be Hybrid EfficientNet Transformer which was 0.97, only smaller than a 0.01 gap. For normal, we found Swin Transformer to have a score of 0.97 and the second score was DenseNet 121 and Hybrid EfficientNet-DOLG, which was 0.94. The other models, including ResNet50 and InceptionNet, also computed comparable results. With respect to recall, the dense architecture of DenseNet worked best on COVID-19 images, and different from precision metric, the hierarchy architecture of Swin Transformer achieved the best results on normal images. The combination of EfficientNet and DOLG took the best place on pneumonia, macro average, and micro average.

Table 6. Comparing results between the five deep learning models on the COVID-19 classification task with respect to recall metric.

Methods	Recall				
	COVID-19	Normal	Pneumonia	Macro-Average	Micro-Average
DenseNet121	0.98	0.94	0.92	0.95	0.95
ResNet50	0.94	0.96	0.89	0.93	0.93
InceptionNet	0.93	0.88	0.94	0.92	0.92
Swin Transformer	0.70	0.97	0.90	0.86	0.82
Hybrid EfficientNet-DOLG	0.97	0.94	0.95	0.96	0.96

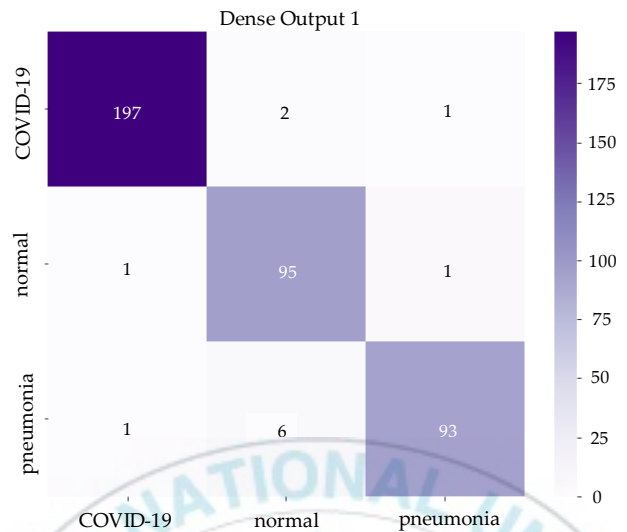
The third metric was the F1-score; in this metric, we could see the pattern that Hybrid EfficientNet produced the best results on all scores except the normal category, in which the top result belonged to DenseNet with a score of 0.95. For COVID-19, pneumonia, macro-average, and micro-average the Hybrid EfficientNet-

DOLG produced the highest results with scores of 0.99, 0.94, 0.95, and 0.96, respectively. For COVID-19, pneumonia, macro-average, and micro-average, the second highest model was DenseNet121, which produced scores of 0.98, 0.93, 0.94, and 0.95 sequentially. Different from precision and recall, the classification performance of DenseNet secured best on normal images, this might be because the dense connections performed well for normal cases regarding the F1-score, then the compound of EfficientNet and DOLG did efficiently on other categories.

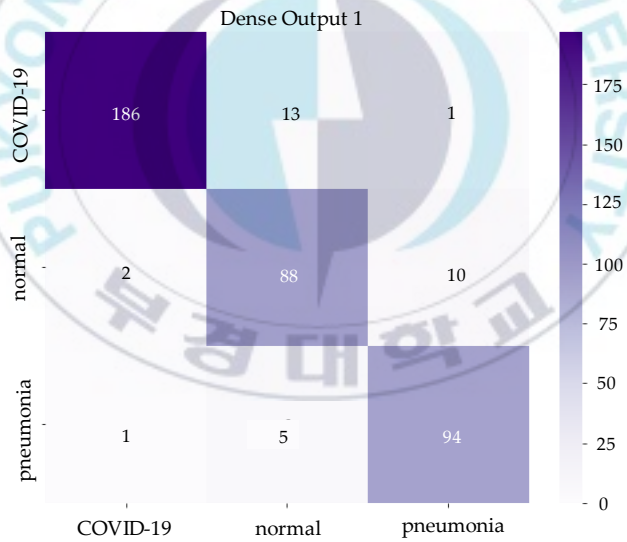
Table 7. Comparing results between the five deep learning models on the COVID-19 classification task with respect to F1-score metric.

Methods	F1-score				
	COVID-19	Normal	Pneumonia	Macro-Average	Micro-Average
DenseNet121	0.98	0.95	0.93	0.94	0.95
ResNet50	0.96	0.89	0.91	0.92	0.93
InceptionNet	0.96	0.85	0.92	0.91	0.92
Swin Transformer	0.82	0.75	0.90	0.82	0.82
Hybrid EfficientNet-DOLG	0.99	0.94	0.94	0.95	0.96

From Table 7, we can conclude that Hybrid EfficientNet-DOLG and DenseNet models are the best models for COVID-19 classification tasks on our customized dataset. Figure 14 and Figure 15 demonstrate the confusion matrix of inference results on the test set and training history of the Hybrid EfficientNet-DOLG and DenseNet models.



(a)



(b)

Fig. 14. Confusion matrix of (a) DenseNet and (b) Hybrid EfficientNet-DOLG on the COVID-19 classification task.

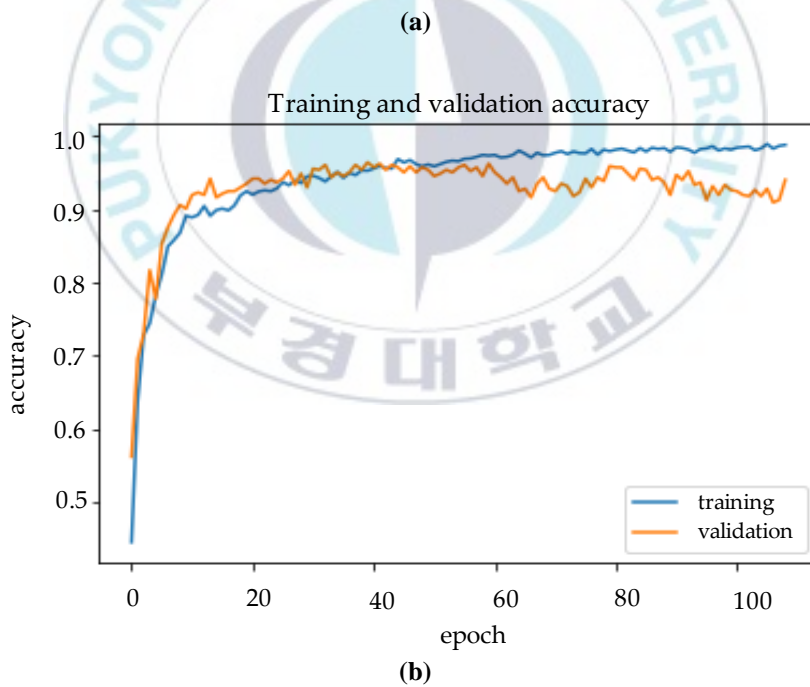
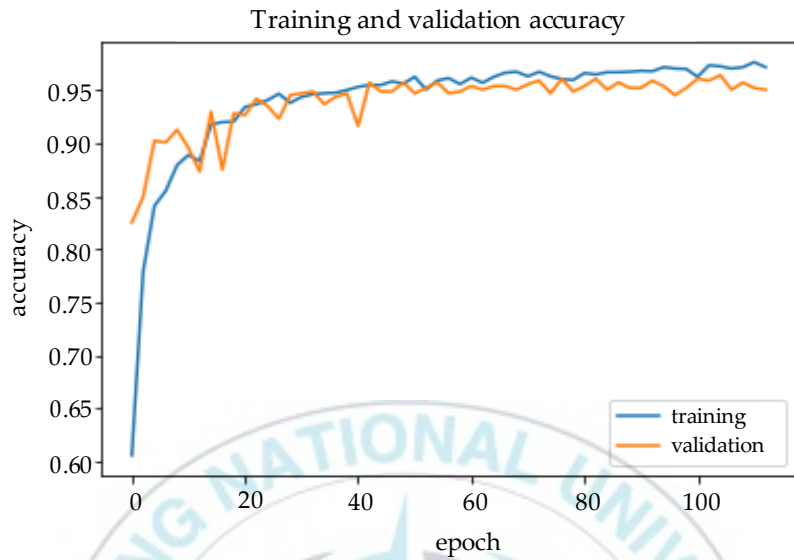


Fig. 15. Training history of (a) DenseNet and (b) Hybrid EfficientNet-DOLG on the COVID-19 classification task.

3.5.2 COVID-19 CT Scan Classification Results

In this paper, we used four deep learning models to run our experiments on COVID-19 detection on a customized dataset. The models we use include, GoogleNet, EfficientNet, Hybrid EfficientNet-DOLG, and DenseNet121.

Table 8. Classification results comparison of four deep learning models on CT Scan Images with respect to Precision metrics

Method	Precision			
	COVID	Normal	Macro-Average	Micro-Average
GoogleNet	0.77	0.75	0.76	0.76
EfficientNet	0.85	0.72	0.79	0.79
Hybrid-EfficientNet-DOLG	0.85	0.81	0.83	0.83
DenseNet121	0.92	0.84	0.88	0.88

From Tables 8, 9 and 10 we can see that DenseNet121 produces the highest score on three evaluation metrics, which are precision, recall, and f1-score. In precision metric, with respect to COVID, the Densenet121 model produced a result of 0.92, then followed by EfficientNet and Hybrid EfficientNet-DOLG with 0.85 accuracies. The same pattern occurred for NORMAL, macro avg, and micro avg, in which the Hybrid EfficientNet-DOLG produced slightly higher results than EfficientNet and GoogleNet.

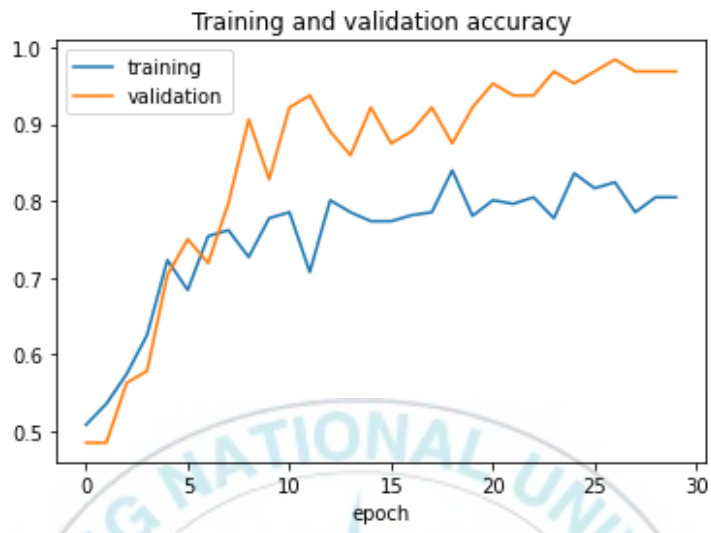
Table 9. Classification results comparison of four deep learning models on CT Scan Images with respect to Recall metrics

Method	Recall			
	COVID	Normal	Macro-Average	Micro-Average
GoogleNet	0.73	0.78	0.76	0.76
EfficientNet	0.66	0.89	0.77	0.77
Hybrid-EfficientNet-DOLG	0.80	0.86	0.83	0.83
DenseNet121	0.82	0.93	0.87	0.88

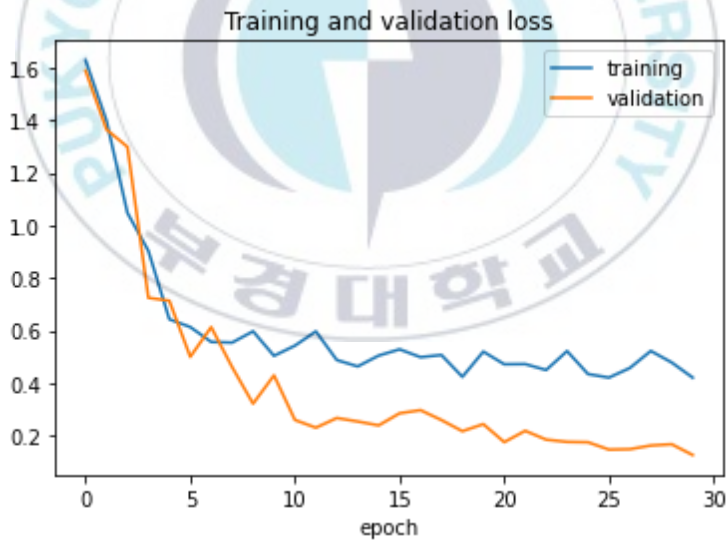
In terms of recall metrics, DenseNet also produced the best results compared to other architecture, with 0.82, 0.93, 0.87, and 0.88 for COVID, NORMAL, micro avg, and macro avg accuracy output respectively, followed by Hybrid EfficientNet-DOLG which also output a comparable result. For the f1-score metric, DensetNet still outperformed on the classification task, Hybrid EfficientNet-DOLG, EfficientNet, and Google also produced comparable results.

Table 10. Classification results comparison of four deep learning models on CT Scan Images with respect to F1-score metrics

Method	F1-score			
	COVID	Normal	Macro-Average	Micro-Average
GoogleNet	0.75	0.76	0.75	0.75
EfficientNet	0.74	0.80	0.77	0.77
Hybrid-EfficientNet-DOLG	0.82	0.83	0.83	0.83
DenseNet121	0.87	0.88	0.87	0.87



(a)



(b)

Fig. 16. Training and validation accuracy (a) loss (b) of DenseNet121.

3.5.3 COVID-19 Chest X-Ray Severity Grading Results

With the COVID-19 severity assessment task, we also trained the customized COVID-19 severity dataset with five models: DenseNet121, ResNet50, InceptionNet, Swin Transformer, and Hybrid EfficientNet-DOLG. The dataset contains images of two categories, level1 and level2, in which level1 indicates the patient severity is normal and the patient can self-quarantine at home without requiring a further treatment response. Level2 indicates that the patients need to have further support and need to go to the hospital for a treatment response because the pneumonia extent of COVID-19 damage is large and severe.

After training models for hours, we obtained the output results as shown in Tables 11-13. We also evaluated severity assessment results on three metrics: precision, recall, and F1-score with respect to level1, level2, macro-average, and micro-average, the same as the COVID-19 classification task. A detailed analysis of deep learning models' performance on COVID-19 severity assessment is presented for each metric under every table.

From Table 11, we can see that with level1, DenseNet121 output had the top precision score result of 0.76, and level2 Hybrid EfficientNet-DOLG produced a precision score of 0.87. The Swin Transformer led the macro-average with a 0.81 precision score, and with respect to the micro-average, the Hybrid Efficient-DOLG also produced the highest score of 0.82. The dense connection of DenseNet helped to reduce gradients vanishing which improve the precision metric of DenseNet on level1 Chest X-Ray images. The Swin Transformer produced the best on macro average because the accuracy of level1 and level2 is very high, and Hybrid EfficientNet-DOLG surpassed other neural nets on micro average because its precision on level2 is the highest and on level1 almost equal DenseNet.

Table 11. Comparing results between the five deep learning models on COVID-19 severity assessment task with respect to precision metric.

Methods	Precision			
	Level1	Level2	Macro-Average	Micro-Average
DenseNet121	0.76	0.84	0.80	0.81
ResNet50	0.74	0.77	0.76	0.76
InceptionNet	0.72	0.77	0.75	0.75
Swin Transformer	0.75	0.86	0.81	0.80
Hybrid EfficientNet-DOLG	0.74	0.87	0.80	0.82

Table 12. Comparing results between the five deep learning models on the COVID-19 severity assessment task with respect to recall metric.

Methods	Precision			
	Level1	Level2	Macro-Average	Micro-Average
DenseNet121	0.67	0.89	0.78	0.81
ResNet50	0.65	0.85	0.70	0.77
InceptionNet	0.70	0.80	0.70	0.76
Swin Transformer	0.72	0.80	0.73	0.75
Hybrid EfficientNet-DOLG	0.75	0.86	0.80	0.82

When comparing the precision score, we could see that the Hybrid EfficientNet-DOLG outperformed on all three categories: level1, macro-average, and micro-average with the score of 0.75, 0.80, and 0.82. The DenseNet121 produced the highest score of level2 (0.89) on the recall metric. The dense connection mechanism

of DenseNet produced is sensitive with level2 Chest X-Ray images that . Swin Transformer and other two convolution-based neural nets, ResNet50 and InceptionNet, also achieved comparable results with DenseNet and Hybrid EfficientNet-DOLG.

Table 13. Comparing results between the five deep learning models on the COVID-19 severity assessment task with respect to F1-score metric.

Methods	Precision			
	Level1	Level2	Macro-Average	Micro-Average
DenseNet121	0.71	0.86	0.79	0.81
ResNet50	0.60	0.84	0.72	0.75
InceptionNet	0.65	0.84	0.75	0.77
Swin Transformer	0.62	0.84	0.63	0.69
Hybrid EfficientNet-DOLG	0.74	0.86	0.80	0.82

The last metric we analyzed was F1-score. In this metric, Hybrid EfficientNet-DOLG outperformed all four categories: level1, level2, macro-average, and micro-average, with scores of 0.74, 0.86, 0.80, and 0.82. The top results on the F1-score of Hybrid EfficientNet-DOLG are based on the robustness of EfficientNet as an encoder of the structure and combine with the global and local descriptor of DOLG. DenseNet also produced high output results with scores of 0.71 on level1, 0.86 on level2, 0.79 on macro-average, and 0.81 on micro-average. Output of DenseNet was only smaller than Hybrid EfficientNet-DOLG with 0.01 score gaps on level1, macro-average, and micro-average and produce the equal result on level2. Other neural nets also achieved comparable results on F1-score with DenseNet and Hybrid EfficientNet-DOLG.

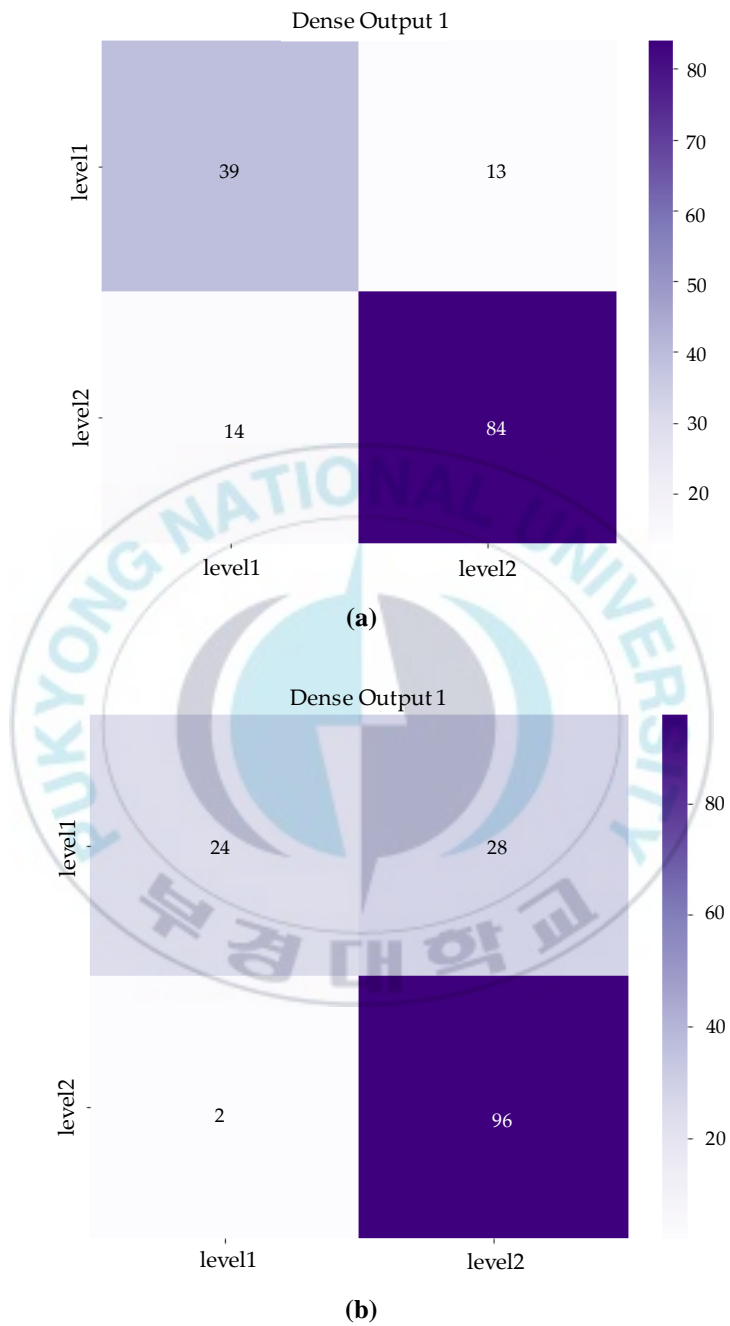
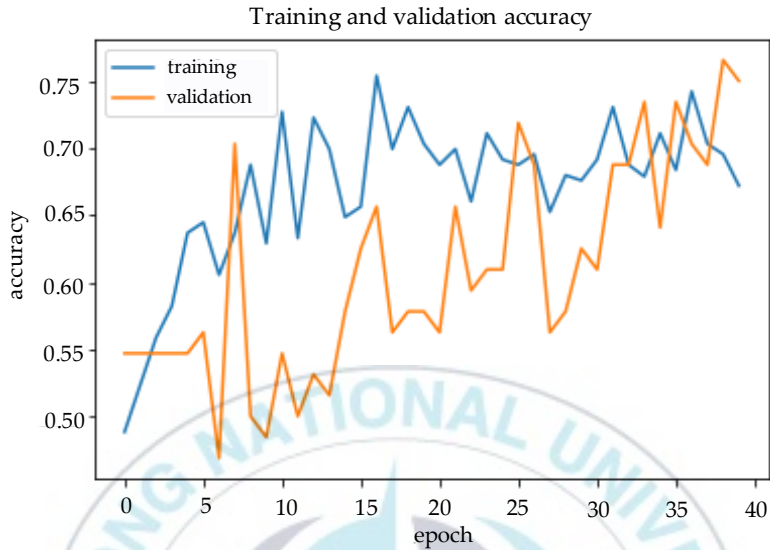
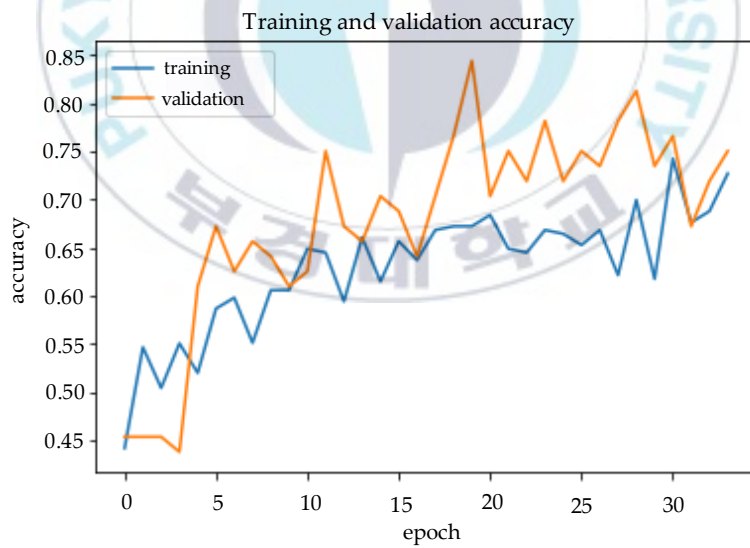


Fig. 17. Confusion matrix of (a) DenseNet and (b) Hybrid EfficientNet-DOLG on the COVID-19 severity assessment task



(a)



(b)

Fig. 18. Training history of (a) DenseNet and (b) Hybrid EfficientNet-DOLG on the COVID-19 severity assessment task

3.5.4 Potential methods and limitations of this study

There are many deep learning architecture and deep transfer learning techniques that could apply to X-Ray and CT Scan imagery as a potential method for classifying COVID-19 detection and severity assessment. Some of the architecture techniques include Wide Residual Networks [53] (WRNs) and Visual Geometry Group (VGG) [54]. Wide Residual Networks are variants of ResNet, which both increase the width and decrease the depth of residual networks, and also create lightweight models with high performance. With only 16 layers, the network can outperform another convolutional neural networks with over 1000 layers on CIFAR and ImageNet datasets.

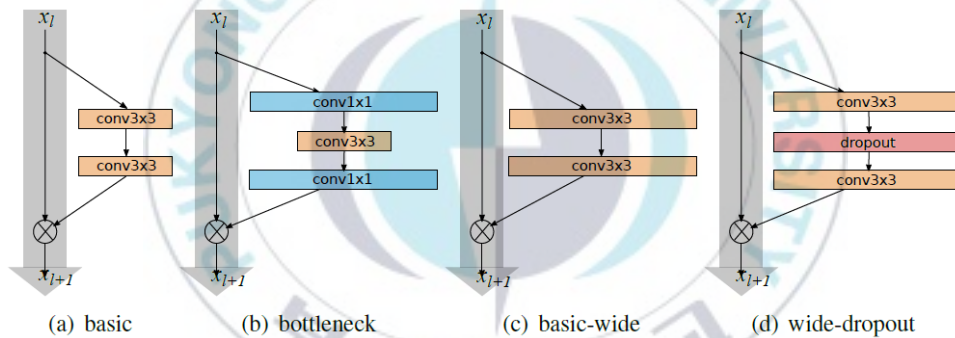


Fig. 19. Wide residual Networks architecture

The second network is VGG, which won the ImageNet Challenge 2014 and was first and second in terms of localization and classification, respectively. We have VGG16 and VGG19, which represent 16 layers and 19 layers of neural networks. In general, the architecture of VGG includes input layers, convolutional layers, hidden layers, and fully connected layers, and depending on the architecture we use, that the number of layers might be different. There is research that studies the application of deep transfer learning, including the work of Naushad et al. [55] in which the author efficiently implemented deep transfer learning techniques for land use and land cover

classification based on WSNs and VGG pre-trained models. Another study by Das et al. [56] tried to apply deep transfer learning automatically to detect COVID-19 based on Chest X-Ray images.

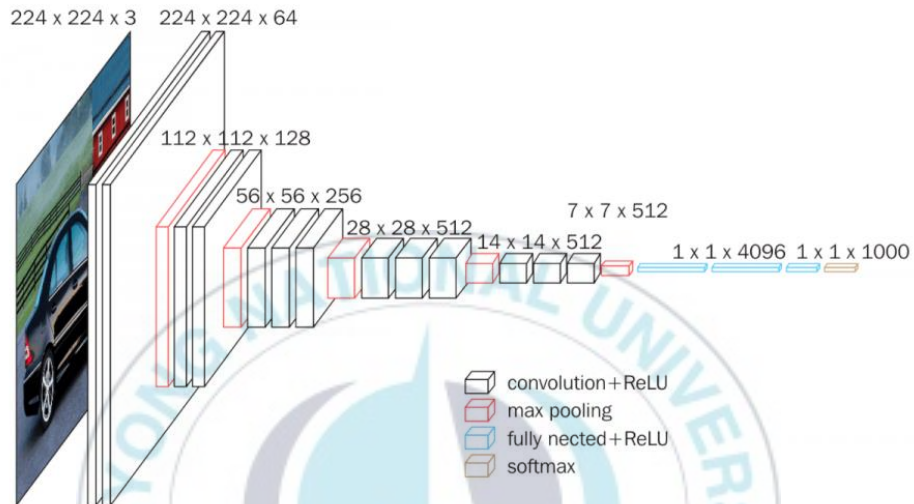


Fig. 20. Visual Geometry Group Net architecture

This study has some limitations. First, we collected data from many open-source datasets; to some extent this might affect the model accuracy. Because X-Ray images obtained from different machines have various image qualities, image color channels as well as resolutions, these factors have significantly impact on the model training pipeline. Another shortcoming of this study was the severity assessment levels; to have a more precise treatment response for patients, having many classes of severity is better than having few classes. In this study, we only focused on two classes, level1 and level2; this is not as detailed as it could be with more levels for severity diagnosis, which means a more appropriate treatment response could be designed. The last disadvantage of this paper is that we did not implement a new deep learning model to customize for our Chest X-Ray and CT Scan dataset. We only used a built-

in model from available libraries, which was then not as efficient as we trained on X-Ray and CT Scan imagery. In future work, we aim to build a model that is lightweight, robust, and has a lower computational complexity for X-Ray image classification tasks. We used six deep neural networks with computational complexity as follows: Swin Transformer (1038 Giga FLOPs), InceptionNet (24.57 Giga FLOPs), Hybrid EfficientNet-DOLG (9.9 Giga FLOPs), DenseNet121 (5.69 Giga FLOPs), EfficientNet B4 (4.2 Giga FLOPs) , and ResNet50 (3.8 Giga FLOPs). We will design a network with computational complexity approximate to 10 Giga FLOPs for an efficient and robust model.



IV. Conclusion

In this thesis, we have demonstrated the advantages of early screening of COVID-19 utilizing CT scan and chest X-ray pictures in order to form a quicker and safer technique of COVID-19 identification. The work mainly taken idea from the paper [57] which published on Applied Sciences journal in January 2022. In order to improve the balance of our training dataset, we also produced new CT Scan and Chest X-Ray datasets from the open datasets that were already accessible. The input data was then cleaned up by getting rid of any poor-quality images. The COVID CXR and Chest X-Ray Pneumonia datasets were combined to create the initial dataset, which was utilized for COVID-19, pneumonia, and normal classification. It had 36,384 pictures in total. The COVID-CT-Dataset, SARS-CoV-2, and COVID-CTSet datasets were combined to create the second dataset, which was utilized for COVID-19 detection through CT scan. Six convolutional and transformer-based deep learning models were the subjects of our investigations. According to the findings, utilizing chest X-ray pictures to identify and rate COVID-19 severity is a promising technique since it yields accurate inference results. The models based on transformers outperformed models based on convolutions in terms of accuracy, recall, and F1-score, as well as other measures.

More data augmentation methods, including GAN [58] will be used in further research to improve the input data used to train training models. In order to enhance model performance for the COVID-19 severity and COVID-19 detection grading tasks, we will additionally take into account tailoring neural network models for the Chest X-Ray and CT Scan dataset. On a research scale, our machine learning model works admirably, but it is not yet ready to be used in production. In the future, we intend to collect additional real case datasets so that we may use our machine learning system to make accurate diagnoses in clinical situations.

References

- [1] Wang, Wenling, Yanli Xu, Ruqin Gao, Roujian Lu, Kai Han, Guizhen Wu, and Wenjie Tan, "Detection of SARS-CoV-2 in different types of clinical specimens," *Jama*, vol. 323, no. 18, pp. 1843-1844, 2020.
- [2] Long, Chunqin, Huaxiang Xu, Qinglin Shen, Xianghai Zhang, Bing Fan, Chuanhong Wang, Bingliang Zeng, Zicong Li, Xiaofen Li, and Honglu Li., "Diagnosis of the Coronavirus disease (COVID-19): rRT-PCR or CT?," *European journal of radiology*, no. 126, p. 108961, 2020.
- [3] Arevalo-Rodriguez, Ingrid, Diana Buitrago-Garcia, Daniel Simancas-Racines, Paula Zambrano-Achig, Rosa Del Campo, Agustin Ciapponi, Omar Sued et al., "False-negative results of initial RT-PCR assays for COVID-19: a systematic review," *PloS one*, vol. 15, no. 12, p. e0242958, 2020.
- [4] Tahamtan, Alireza, and Abdollah Ardebili., "Real-time RT-PCR in COVID-19 detection: issues affecting the results," *Real-time RT-PCR in COVID-19 detection: issues affecting the results*, vol. 20, no. 5, pp. 453-454, 2020.
- [5] B. van Ginneken, "The potential of artificial intelligence to analyze chest radiographs for signs of COVID-19 pneumonia," *Radiology*, vol. 299, no. 1, p. E214, 2021.
- [6] Khanna, Munish, Astitwa Agarwal, Law Kumar Singh, Shankar Thawkar, Ashish Khanna, and Deepak Gupta, "Radiologist-level two novel and robust automated computer-aided prediction models for early detection of COVID-19 infection from chest X-ray images," *Arabian Journal for Science and Engineering*, pp. 1-33, 2021.
- [7] Le Dinh, Tuan, Seong-Geun Kwon, Suk-Hwan Lee, and Ki-Ryong Kwon, "A Study on Vision Transformer for Medical Image Segmentation," in *Journal of Korean Information Science Society*, 2021.
- [8] Le Dinh, Tuan, Suk-Hwan Lee, Seong-Geun Kwon, and Ki-Ryong Kwon, "Cell Nuclei Segmentation in Cryonuseg dataset using Nested Unet with EfficientNet Encoder," in *International Conference on Electronics, Information, and Communication*, 2022.
- [9] Gozes, Ophir, Maayan Frid-Adar, Hayit Greenspan, Patrick D. Browning, Huangqi Zhang, Wenbin Ji, Adam Bernheim, and Eliot Siegel., "Rapid ai development cycle for the coronavirus (covid-19) pandemic: Initial results for automated detection & patient monitoring using deep learning ct image analysis," *arXiv preprint arXiv:2003.05037*, 2020.
- [10] Narin, Ali, Ceren Kaya, and Ziyet Pamuk., "Automatic detection of coronavirus disease (covid-19) using x-ray images and deep convolutional

- neural networks," *Pattern Analysis and Applications*, vol. 24, no. 3, pp. 1207-1220, 2021.
- [11] Rehman, Amjad, Tanzila Saba, Usman Tariq, and Noor Ayesha, "Deep learning-based COVID-19 detection using CT and X-ray images: Current analytics and comparisons," *IT professional*, vol. 23, no. 3, pp. 63-68, 2021.
- [12] Tang, Shanjiang, Chunjiang Wang, Jiangtian Nie, Neeraj Kumar, Yang Zhang, Zehui Xiong, and Ahmed Barnawi., "EDL-COVID: Ensemble deep learning for COVID-19 case detection from chest X-ray images," *IEEE Transactions on Industrial Informatics*, vol. 17, no. 9, pp. 6539-6549, 2021.
- [13] Ohata, Elene Firmeza, Gabriel Maia Bezerra, Joao Victor Souza das Chagas, Aloísio Vieira Lira Neto, Adriano Bessa Albuquerque, Victor Hugo C. de Albuquerque, and Pedro Pedrosa Reboucas Filho., "Automatic detection of COVID-19 infection using chest X-ray images through transfer learning," *IEEE/CAA Journal of Automatica Sinica* , vol. 8, no. 1, pp. 239-248, 2020.
- [14] Horry, Michael J., Subrata Chakraborty, Manoranjan Paul, Anwaar Ulhaq, Biswajeet Pradhan, Manas Saha, and Nagesh Shukla., "COVID-19 detection through transfer learning using multimodal imaging data," *Ieee Access*, vol. 8, pp. 149808-149824, 2020.
- [15] Wang, Linda, Zhong Qiu Lin, and Alexander Wong., "Covid-net: A tailored deep convolutional neural network design for detection of covid-19 cases from chest x-ray images," *Scientific Reports*, vol. 10, no. 1, pp. 1-12, 2020.
- [16] E. Irmak, "COVID-19 disease severity assessment using CNN model," *IET image processing*, vol. 15, no. 8, pp. 1814-1824, 2021.
- [17] Orsi, Marcello A., Giancarlo Oliva, Tahereh Toluian, Carlo Valenti Pittino, Marta Panzeri, and Michaela Cellina., "Feasibility, reproducibility, and clinical validity of a quantitative chest X-ray assessment for COVID-19," *he American journal of tropical medicine and hygiene*, vol. 103, no. 2, p. 822, 2020.
- [18] Liang, Wenhua, Jianhua Yao, Ailan Chen, Qingquan Lv, Mark Zanin, Jun Liu, SookSan Wong et al., "Early triage of critically ill COVID-19 patients using deep learning," *Nature communications*, vol. 11, no. 1, pp. 1-7, 2020.
- [19] Liang, Wenhua, Hengrui Liang, Limin Ou, Binfeng Chen, Ailan Chen, Caichen Li, Yimin Li et al., "Development and validation of a clinical risk score to predict the occurrence of critical illness in hospitalized patients with COVID-19," *AMA internal medicine*, vol. 180, no. 8, pp. 1081-1089, 2020.
- [20] Colombi, Davide, Flavio C. Bodini, Marcello Petrini, Gabriele Maffi, Nicola Morelli, Gianluca Milanese, Mario Silva, Nicola Sverzellati, and Emanuele Michieletti., "Well-aerated lung on admitting chest CT to predict adverse

- outcome in COVID-19 pneumonia," *Radiology*, vol. 296, no. 2, pp. E86-E96, 2020.
- [21] Wong, A., Lin, Z.Q., Wang, L. et al., "Towards computer-aided severity assessment via deep neural networks for geographic and opacity extent scoring of SARS-CoV-2 chest X-rays," *Scientific reports*, vol. 11, no. 1, pp. 1-8, 2021.
- [22] Jacobi, Adam, Michael Chung, Adam Bernheim, and Corey Eber., "Portable chest X-ray in coronavirus disease-19 (COVID-19): A pictorial review," *Clinical imaging*, vol. 64, pp. 35-42, 2020.
- [23] Cozzi, Diletta, Marco Albanesi, Edoardo Cavigli, Chiara Moroni, Alessandra Bindi, Silvia Luvarà, Silvia Lucarini, Simone Busoni, Lorenzo Nicola Mazzoni, and Vittorio Miele., "Chest X-ray in new Coronavirus Disease 2019 (COVID-19) infection: findings and correlation with clinical outcome," *La radiologia medica*, vol. 125, no. 8, pp. 730-737, 2020.
- [24] Li, Yan, and Liming Xia, "Coronavirus disease 2019 (COVID-19): role of chest CT in diagnosis and management," *Ajr Am J Roentgenol*, vol. 214, no. 6, pp. 1280-1286, 2020.
- [25] Rousan, Liqa A., Eyhab Elobeid, Musaab Karrar, and Yousef Khader, "Chest x-ray findings and temporal lung changes in patients with COVID-19 pneumonia," *BMC Pulmonary Medicine*, vol. 20, no. 1, pp. 1-9, 2020.
- [26] Dong, Ensheng, Hongru Du, and Lauren Gardner, "An interactive web-based dashboard to track COVID-19 in real time," *The Lancet infectious diseases*, vol. 20, no. 5, pp. 533-534, 2020.
- [27] Ortiz, Anthony, Anusua Trivedi, Jocelyn Desbiens, Marian Blazes, Caleb Robinson, Sunil Gupta, Rahul Dodhia et al., "Effective deep learning approaches for predicting COVID-19 outcomes from chest computed tomography volumes," *Scientific reports*, vol. 10, no. 1, pp. 1-10, 2022.
- [28] Javaheri, Tahereh et al., "CovidCTNet: an open-source deep learning approach to diagnose covid-19 using small cohort of CT images," *NPJ digital medicine*, vol. 4, no. 1, p. 29, 2021.
- [29] Afshar, P., Rafiee, M.J., Naderkhani, F. et al., "Human-level COVID-19 diagnosis from low-dose CT scans using a two-stage time-distributed capsule network," *Scientific Reports*, p. 4827, 2022.
- [30] Lee, Edward H et al., "Deep COVID DeteCT: an international experience on COVID-19 lung detection and prognosis using chest CT," *NPJ digital medicine*, vol. 4, no. 1, p. 11, 2021.
- [31] Khan, Asif Iqbal et al., "CoroNet: A deep neural network for detection and diagnosis of COVID-19 from chest x-ray images," *Computer methods and programs in biomedicine*, vol. 196, no. 105581, 2020.

- [32] Roberts, M. et al. , "Common pitfalls and recommendations for using machine learning to detect and prognosticate for COVID-19 using chest radiographs and CT scans," *Nature Machine Intelligence*, vol. 3, p. 199–217, 2021.
- [33] Kermany, Daniel S et al., "Identifying Medical Diagnoses and Treatable Diseases by Image-Based Deep Learning," *Cell* , vol. 172, no. 5, pp. 1122-1131, 2018.
- [34] Ucar, Ferhat, and Deniz Korkmaz, "COVIDiagnosis-Net: Deep Bayes-SqueezeNet based diagnosis of the coronavirus disease 2019 (COVID-19) from X-ray images," *Medical hypotheses*, vol. 140, no. 109761, 2020.
- [35] Jia Wu, Xiu-Yun Chen, Hao Zhang, Li-Dong Xiong, Hang Lei, Si-Hao Deng., "Hyperparameter Optimization for Machine Learning Models Based on Bayesian Optimization," *Journal of Electronic Science and Technology*, vol. 17, no. 1, pp. 26-40, 2019.
- [36] Wong, A et al., "Towards computer-aided severity assessment via deep neural networks for geographic and opacity extent scoring of SARS-CoV-2 chest X-rays," *Scientific reports*, vol. 11, no. 1, p. 9315, 2021.
- [37] Cohen, Joseph Paul et al, "Predicting COVID-19 Pneumonia Severity on Chest X-ray With Deep Learning," *Cureus*, vol. 12, no. 7, p. e9448, 2020.
- [38] Zhao, Jinyu, Yichen Zhang, Xuehai He, and Pengtao Xie., "Covid-ct-dataset: a ct scan dataset about covid-19," *arXiv preprint arXiv:2003.13865* 490, 2020.
- [39] Angelov, Plamen, and Eduardo Almeida Soares, "SARS-CoV-2 CT-scan dataset: A large dataset of real patients CT scans for SARS-CoV-2 identification," *MedRxiv*, 2020.
- [40] Rahimzadeh, M., Attar, A., & Sakhaei, S. M, "A fully automated deep learning-based network for detecting covid-19 from a new and large lung ct scan dataset," *Biomedical Signal Processing and Control*, vol. 68, p. 102588, 2021.
- [41] Huang, Gao, Zhuang Liu, Laurens Van Der Maaten, and Kilian Q. Weinberger, "Densely connected convolutional networks," in *Proceedings of the IEEE conference on computer vision and pattern recognition*, 2017.
- [42] He, Kaiming, Xiangyu Zhang, Shaoqing Ren, and Jian Sun, "Deep residual learning for image recognition," in *Proceedings of the IEEE conference on computer vision and pattern recognition*, 2016.
- [43] Szegedy, Christian, Wei Liu, Yangqing Jia, Pierre Sermanet, Scott Reed, Dragomir Anguelov, Dumitru Erhan, Vincent Vanhoucke, and Andrew Rabinovich, "Going deeper with convolutions," in *Proceedings of the IEEE conference on computer vision and pattern recognition*, 2015.

- [44] Liu, Ze, Yutong Lin, Yue Cao, Han Hu, Yixuan Wei, Zheng Zhang, Stephen Lin, and Baining Guo, "Swin transformer: Hierarchical vision transformer using shifted windows," in *Proceedings of the IEEE/CVF International Conference on Computer Vision*, 2021.
- [45] Tan, Mingxing, and Quoc Le, "Efficientnet: Rethinking model scaling for convolutional neural networks," in *International conference on machine learning*, 2019.
- [46] Howard, Andrew G., et al., "Mobilenets: Efficient convolutional neural networks for mobile vision applications," *arXiv preprint arXiv:1704.04861*, 2017.
- [47] He, Kaiming, Xiangyu Zhang, Shaoqing Ren, and Jian Sun, "Deep residual learning for image recognition," in *In Proceedings of the IEEE conference on computer vision and pattern recognition*, 2016.
- [48] C. Henkel, "Efficient large-scale image retrieval with deep feature orthogonality and Hybrid-Swin-Transformers," *arXiv preprint arXiv:2110.03786*, 2021.
- [49] Yang, Min, Dongliang He, Miao Fan, Baorong Shi, Xuotong Xue, Fu Li, Errui Ding, and Jizhou Huang, "Dolg: Single-stage image retrieval with deep orthogonal fusion of local and global features," in *Proceedings of the IEEE/CVF International Conference on Computer Vision*, 2021.
- [50] Bassi, Pedro RAS, and Romis Attux., "A deep convolutional neural network for COVID-19 detection using chest X-rays," *Research on Biomedical Engineering*, vol. 38, no. 1, pp. 139-148, 2022.
- [51] Nishio, Mizuho, Shunjiro Noguchi, Hidetoshi Matsuo, and Takamichi Murakami, ""Automatic classification between COVID-19 pneumonia, non-COVID-19 pneumonia, and the healthy on chest X-ray image: combination of data augmentation methods," *Scientific reports*, vol. 10, no. 1, pp. 1-6, 2020.
- [52] Kingma Diederik, P., and Jimmy Ba Adam, "A method for stochastic optimization," *arXiv preprint arXiv:1412.6980*, 2014.
- [53] Zagoruyko, Sergey, and Nikos Komodakis, "Wide residual networks," *arXiv preprint arXiv:1605.07146*, 2016.
- [54] Simonyan, Karen, and Andrew Zisserman, "Very deep convolutional networks for large-scale image recognition," *arXiv preprint arXiv:1409.1556*, 2014.
- [55] Naushad, Raoof, Tarunpreet Kaur, and Ebrahim Ghaderpour, "Deep transfer learning for land use and land cover classification: A comparative study," *Sensors*, vol. 21, no. 23, p. 8083, 2021.

- [56] Das, N. Narayan, Naresh Kumar, Manjit Kaur, Vijay Kumar, and Dilbag Singh, "Automated deep transfer learning-based approach for detection of COVID-19 infection in chest X-rays," *Irbm*, 2020.
- [57] Le Dinh, Tuan, Suk-Hwan Lee, Seong-Geun Kwon, and Ki-Ryong Kwon, "COVID-19 Chest X-ray Classification and Severity Assessment Using Convolutional and Transformer Neural Networks," *Applied Sciences*, vol. 12, no. 10, p. 4861, 2022.
- [58] Goodfellow Ian, J., Pouget-Abadie Jean, Mirza Mehdi, Xu Bing, Warde-Farley David, Ozair Sherjil, and C. Courville Aaron, "Generative adversarial nets," in *Proceedings of the 27th international conference on neural information processing systems*, 2014.



Acknowledgement

This thesis would not have been completed without the supports and help from people around me. First of all, I would like to thank my advisor, **Prof. Ki-Ryong Kwon**, for the patient guidance, encouragement and advice he has provided throughout my time as his student. I have been extremely lucky to have an advisor who cared so much about my work, and who responded to my questions and queries so promptly. I am so grateful for his endless help and care what he has given to me. I would also like to thank my co-advisors, **Prof. Suk-Hwan Lee** and **Prof. Seong-Geun Kwon**, for their useful comments and suggestions that helped me to revise this thesis. Furthermore, I would also like to express my sincere gratitude to my lab seniors: **Dr. Jin-Hyeok Park**, **Dr. Long Hoang**, and **Mr. Khurshid Farkhodov**; also my lab mates: **Mr. Rashid MD Mamunur**, **Mr. Nhan Tran**, **Mr. Kim Jae-Hyun**, and **Mr. Thuan Tran**, they gave me lots of useful suggestions and comments, experience, knowledge, and helped me in difficult situations during the study period. Moreover, I am very grateful to all the students from Vietnam at PKNNU with whom I have had the pleasure to study here in Busan.

Finally, it should be noted that nobody has been more important to me in the pursuit of graduate studies than the members of my family. I would like to thank my parents, whose love and guidance are with me in whatever I pursue. Most importantly, I would like to thank my loving and supportive wife, who has provided endless inspiration.